2016

Determining the effect of knocking out microRNA-21 on subsarcolemmal and interfibrillar mitochondria

Madhur Batra
Virginia Commonwealth University

Determining the effect of knocking out microRNA-21 on subsarcolemmal and interfibrillar mitochondria

A thesis submitted in partial fulfillment of the requirements for the degree of Master of Science in Physiology & Biophysics at Virginia Commonwealth University.

By

Madhur Batra
B.S., Virginia Commonwealth University, Richmond, VA, 2014

Director: Dr. Edward J. Lesnefsky, M.D.
Professor of Internal Medicine
VCU School of Medicine

Virginia Commonwealth University
Richmond, Virginia
May 2016

Table of Contents

Acknowledgement

I would like to thank my family and friends, who provided me with endless support and encouragement. I sincerely appreciate Dr. Edward Lesnefsky, Dr. Fadi Salloum, Dr. Robert Diegelmann, Dr. Roland Pittman, Dr. Qun Chen, and Jeremy Thompson for their direction and guidance throughout this project.

List of Figures and Tables

List of Abbreviations

ADP – Adenosine diphosphate
ANOVA – Analysis of variance
ATP – Adenosine triphosphate
cCS – Crude cytosol
CP1 – Chapell-Perry 1
CP2 – Chapell-Perry 2
CRC – Calcium Retention Capacity
CVD – Cardiovascular disease
DKO – Double knockout
DNP – 2.4-dinitrophenol
EGTA – Ethylene glycol-bis(2-aminoethylether)-N,N,N'N'-tetraacetic acid
HRP – Horseradish Peroxidase
IFM – Interfibrillar mitochondria
IMM – Inner mitochondrial membrane
IMS – Inner mitochondrial space
KME – 100mM KCl, 50mM MOPS, 0.5mM EGTA
MOPS – 3-(N-morpholino) propanesulfonic acid
RCR – Respiratory control ratio
ROS – Reactive oxygen species
MPTP – Mitochondrial permeability transition pore
PDCD4 – Programmed cell death 4
PH – Polytron Homogenate
PP – Polytron Pellet
PTEN – Phosphatase and tensin homolog deleted in chromosome 10
SEM – Standard error of mean
SSM – Subsarcolemmal mitochondria
STZ – Streptozotocin
T2DM – Type 2 diabetes mellitus
TGFRBII – Transforming growth factor, beta receptor II
TMRM – Tetramethylrhodamine methyl ester
TMPD – N,N,N',N'-tetramethyl-*p*-phenylenediamine
WT – Wild type

Abstract

DETERMINING THE EFFECT OF KNOCKING OUT MICRORNA-21 ON CARDIAC SUBSARCOLEMMAL AND INTERFIBRILLAR MITOCHONDRIA

By Madhur Batra, B.S.

A thesis submitted in partial fulfillment of the requirements for the degree of Master of Science in Physiology & Biophysics at Virginia Commonwealth University.

Virginia Commonwealth University, Richmond, VA, 2016

Director: Dr. Edward J. Lesnefsky, M.D.
Professor of Internal Medicine
VCU School of Medicine

Type 2 diabetes mellitus is a growing problem across the world and has significant pathological changes associated with it, including diabetic cardiomyopathy, wherein cardiac function is reduced. MicroRNA-21 has been shown to play a role in both the heart and diabetes so it was thought that knocking out miR-21 could have a protective effect on oxidative phosphorylation function in diabetic mice. Subsarcolemmal and interfibrillar mitochondria were isolated from adult male WT, miR-21 KO, db/db, and double knockout mice (db/db and miR-21 KO cross) and evaluated for function. Knocking out miR-21 in diabetic mice showed a restorative effect in Complex I and Complex II function even though it increased ROS production in Complex I and did not show a significant change in MPTP opening. Knocking out miR-21 could potentially restore oxidative phosphorylation function in diabetic patients but at the expense of producing more ROS.

Chapter 1: Introduction

1.1 Mitochondria

Mitochondria are the primary organelles involved in energy production and are critical for proper cellular function. Enzymes in the mitochondria oxidize carbohydrates, fats, and amino acids and the energy released in these processes generates Adenosine Triphosphate (ATP), which is the major energy molecule of cells (Cox & Nelson, 2000). This overall process is referred to as oxidative phosphorylation. Electrons are first transferred to electron acceptors, which then pass the electrons through a chain of membrane bound carrier molecules, most of which are integral proteins in the inner mitochondrial membrane (IMM). Complex I of the respirasome is also known as NADH dehydrogenase. NADH is oxidized by ubiquinone and in the process, four protons are transferred to the intermembrane space (IMS). Complex II is also called succinate dehydrogenase. Succinate is oxidized to fumarate and ubiquinone again is reduced however no protons are transferred to the IMS in this reaction. Complex III, or cytochrome c reductase, oxidizes one molecule of reduced ubiquinone molecule, or ubiquinol, and reduces two cytochrome c molecules. Cytochrome c can only accept one electron at a time so this reaction occurs in two steps, all while pumping protons into the IMS. Complex IV, also known as cytochrome c oxidase, is the last protein in the electron transport chain and transfers electrons to oxygen and also transfers protons to the IMS.(Cox & Nelson, 2000). These four complexes make up the electron transport chain (ETC). The electron transfer activity of this chain is coupled with the pumping of protons across the IMM, which creates a concentration difference and separation of charge,

jointly called the proton-motive force, across the inner mitochondrial membrane. This force is the foundation for ATP synthesis. Proton specific pores in the IMM are attached to ATP Synthase, or Complex V, molecules. As protons passively move down their concentration gradient back into the mitochondrial matrix, ATP Synthase is able to phosphorylate Adenosine Diphosphate (ADP) into an ATP molecule. ATP molecules can then be used as energy carrier molecules for the cell (Cox & Nelson, 2000). Since the heart needs to pump constantly to provide blood to tissues throughout the body, it should be no surprise that heart muscle has a high concentration of mitochondria. In pathological states such as diabetes mellitus, cardiac mitochondria and, subsequently, cardiac function can be adversely affected (Marin-Garcia, 2013).

During respiration, different terms are used to describe the various points of oxidative phosphorylation and they can be measured to determine the function of the respirasome in mitochondria. State 2 respiration occurs after mitochondria and substrates for oxidation have been added but no ATP is being produced. State 3 respiration is triggered after the addition of ADP; ATP is produced and oxygen is consumed in the process. When the ADP has been converted to ATP, oxygen consumption slows and this signifies State 4 respiration. The respiratory control ratio (RCR) is the ratio of State 3 respiration to State 4 respiration and links the phosphorylation of ADP to the consumption of oxygen. The ADP:O ratio signifies how much oxygen is necessary to phosphorylate a known quantity of ADP. Adding additional ADP shows the maximum coupled respiration rate. The addition of a protonophore to uncouple the flow of protons across the IMM from ATP synthesis is

used to measure the maximum uncoupled respiration rate (Lesnefsky and Hoppel, 2006).

The mitochondrial permeability transition pore (MPTP) is a protein pore that forms in the IMM during pathological conditions and can contribute to cell death. The MPTP opening has been implicated in increasing cell death after ischemia-reperfusion injury (Wong, Steenbergen, & Murphy, 2012). Studies have shown that calcium is a key factor in MPTP opening and once the mitochondria loses the ability to sequester calcium and maintain homeostasis, MPTP opening can occur, which can lead to cell death (Baumgartner et al., 2009). In our study, calcium retention capacity was used as a proxy to study MPTP opening in the different test groups.

1.1.1 Subsarcolemmal and Interfibrillar Mitochondria

There are two distinct populations of mitochondria that exist in cardiac myocytes: subsarcolemmal mitochondria (SSM) and interfibrillar mitochondria (IFM). As the names imply, SSM are located underneath the sarcolemma and IFM are located in between the contractile elements. Not only do these mitochondrial populations differ in location, but also in biochemical properties, which causes them to respond differently to physiological and pathological changes. Williamson et al. (2010) showed that SSM and IFM respond differently to streptozotocin (STZ)-induced diabetes and that IFM had a higher tendency to undergo apoptosis in the type 1 diabetic state (Williamson et al., 2010). Subsarcolemmal mitochondria, in skeletal muscle, have also been shown to have a lower rate of efficiency than interfibrillar mitochondria when producing ATP (Mollica et al., 2006). Specifically in cardiac muscle, IFM were shown to utilize all substrates in oxidative

phosphorylation faster than in SSM (Palmer, Tandler, & Hoppel, 1977). Since subsarcolemmal and interfibrillar mitochondria respond differently to pathologic states, such as diabetes, we thought it would be prudent to check the function of both mitochondrial populations in the heart.

1.2 Type 2 Diabetes Mellitus and Diabetic Cardiomyopathy

Type 2 diabetes mellitus (T2DM) is characterized by the body's resistance to the effects of insulin. This long-term syndrome progresses as the body tries to overcompensate for the ineffective use of insulin by liver, fat, and muscle cells by producing more and more insulin. Eventually, even the increased levels of insulin are not enough to keep the blood glucose levels in check. Because the pathology has a long timespan, symptoms may have a delayed onset (National Institute for of Diabetes and Digestive and Kidney Diseases [NIDDK], 2014). Type 2 diabetes is more common than type 1 diabetes and as of 2010, approximately 285 million people across the world were affected by type 2 diabetes (Melmed, Polonsky, Larsen, & Kronenberg, 2011). There are many risk factors for T2DM, including gene susceptibility and increased glucose production, but the main cause is obesity and lack of physical exercise. Physical inactivity can lead to obesity, which can cause insulin resistance. Since obesity can also lead to other pathological states, such as cardiovascular disease and osteoarthritis, it is important to reduce body weight to a manageable level to help control insulin resistance (NIDDK, 2014).

1.2.1 Diabetic Cardiomyopathy

Diabetic cardiomyopathy is a catch all term used to describe the amalgamation of different cardiac pathological states, some of which fall under the category of cardiovascular disease (CVD), for patients suffering from diabetes. Type 2 diabetes is a strong risk factor for CVD, which is actually the main cause of mortality of patients suffering from T2DM. Diabetic patients have a higher incidence of hypertension, obesity, and dyslipidemia than the normal population and all of these pathologies are independent risk factors for diabetic cardiomyopathy. Diabetic patients also show increased reactive oxygen species (ROS) production, which can cause damage to DNA and other subcellular structures, eventually leading to cell damage and improper function. Hyperglycemia can lead to glucose autooxidation, which causes mitochondria to produce ROS in excess (Boudina & Abel, 2010). This can have adverse effects on cardiac function as mitochondria make up a good portion of cardiomyocytes. This oxidative stress can also cause imbalances in calcium homeostasis, which may lead to further cardiac dysfunction (Clark, 2007). Diabetic cardiomyopathy has also been known to cause contractile dysfunction and alter energy metabolism in the heart. In a db/db mouse model, oxidative phosphorylation rates were shown to be less than in control mice and production of ROS was shown to be higher (Aluri, Koka, Lesnefsky, & Kukreja, 2012). Specifically in SSM and IFM, diabetic hearts showed lower Complex I, II, and III activity, in certain measures, and superoxide production was shown to be higher in diabetic IFM (Williamson et al., 2009).

1.3 microRNA-21

MicroRNAs (miRNAs) are small, noncoding nucleotide strands that serve to repress gene expression by degrading mRNA strands and inhibiting translation (Cheng & Zhang, 2010). MicroRNA-21 (miR-21), specifically, has been found to be overexpressed in many solid tumors and is considered an onco-miR, or a microRNA molecule associated with cancer. Since miR-21 acts to repress the activity of tumor suppressors such as PDCD4 and TGFBRII, it has been implicated in breast cancer, colon cancer, and lung cancer, among others (Asangani et al., 2008; Iorio et al., 2005; Volina et al., 2006). With regards to cardiac disease, studies have shown that miR-21 has variable effects depending on the pathological state and the type of cell in question. Cardiac hypertrophy is a normal compensatory mechanism that occurs in response to some disease states, such as hypertension, and in hypertrophic hearts miR-21 was found to be upregulated (Tu et al., 2013). Specifically in fibroblasts, miR-21 expression was higher than in cardiomyocytes and this led to fibrosis, which is a poor outcome and leads to worse function of the heart. Fibroblasts are non-contractile cells in the heart and contribute by producing collagen and other fibers. Inhibiting miR-21 activity in fibroblasts led to reduced fibrosis and increased cardiac function, including a decrease in left ventricular hypertrophy compared to control mice (Thum et al., 2008). In myocardial infarction studies, miR-21 was found to be overexpressed in border areas of infarcted hearts and underexpressed in infarcted areas. Increasing expression of miR-21, via hydrogen sulfide application, led to a decrease in infarct size (Toldo et al., 2014). This result carries significance with regards to diabetes since H_2S has been shown to affect diabetic

cardiomyopathy as well. In a type 1 diabetes model, H_2S was found to decrease fibrosis in the heart and also reduce hypertrophy (Szabo, 2012). MicroRNA-21 has been studied in context with T2DM as well. A characteristic sign of type 2 diabetes mellitus is hyperglycemia, or high blood glucose levels. This pathologic state can eventually lead to hypertrophy in the kidney, which can cause kidney failure. This pathway is partly caused by the repressed expression of phosphatase and tensin homolog deleted in chromosome 10 (PTEN), a tumor suppressor protein. In the hyperglycemic state, decreased PTEN levels were shown to be caused by increased miR-21 expression. Inhibiting endogenous miR-21 expression allowed for normal expression of PTEN and decreased kidney hypertrophy (Dey et al., 2011). Another study implicated miR-21 in diabetic renal disease and showed that upregulating miR-21 led to increased fibrosis and worse renal function when compared to baseline (McClelland et al., 2015). MicroRNA-21 expression was also found to be upregulated in fibroblasts in diabetic cardiomyopathic patient hearts and was thought to increase cardiac fibrosis in diabetic hearts (Kumar, Raut, Saika, Sharma, & Khullar, 2011).

1.4 Rationale for Present Study

Since T2DM is a growing issue in countries across the world, it is important to expand the base of knowledge that exists on this pathology so that we may better help patients that have type 2 diabetes mellitus. Decreasing microRNA-21 expression has been shown to have positive effects on diabetic pathologies and certain cardiac states so we thought there might be a link with miR-21 and diabetic

cardiomyopathy. We hypothesized that knocking out miR-21 would lead to some restoration of cardiac function, in terms of oxidative phosphorylation, calcium homeostasis, and ROS production, when compared to type 2 diabetic mice. We compared four groups of mice: C57BL/6J, miR-21 knockout (KO), db/db (T2DM model), and a double knockout (DKO) strain (mir-21 KO and db/db cross). The db/db mouse model is characterized by a deficiency in the leptin receptor, which causes the mouse to develop obesity and type 2 diabetes with the progression of age (Belke & Seveson, 2012). Therefore, in terms of cardiac pathology, it has served as the distinctive model to study diabetic cardiomyopathy and is why it was chosen for this study.

To see if there were any significant differences in function, the activity of subsarcolemmal and interfibrillar mitochondria were checked by comparing oxidative phosphorylation rates of Complex I, Complex II, and Complex IV, H_2O_2 production, calcium retention capacity, and membrane potential among the four test groups.

Chapter 2: Materials and Methods

2.1 Materials

2.1.1. Chemicals and Reagents

Chemicals and reagents were either purchased from Sigma-Aldrich, Saint Loius, MO, for mitochondrial isolation and functional assays, or from Fisher Scientific, Pittsburgh, PA.

2.1.2. Animals

C57BL/6J (WT)(n=5) and homozygous Lepr^{db} (db/db)(n=4) mice were purchased from The Jackson Laboratory, Bar Harbor, Maine. The miR-21 KO mice (n=6) were obtained from Eric Olson's laboratory at the University of Texas Southwestern Medical Center (Patrick et al., 2010). The DKO mice(n=6) were generated by cross breeding the miR-21 KO mice with the db/db mice. All mice were aged eight to twelve weeks through the Division of Animal Resources (DAR) of Virginia Commonwealth University (VCU). All mice were housed in a fully AALAC-accredited Animal Research Facility at VCU. All procedures that were implemented followed the National Institutes of Health guidelines for the humane use and care of laboratory animals for biomedical research. All protocols were reviewed and approved by the Institutional Animal Care and Use Committee (IACUC) of VCU.

2.2 Methods

2.2.1 Isolation of heart tissue homogenates, cytosol, subsarcolemmal mitochondria, and interfibrillar mitochondria

Male mice were anesthetized with sodium pentobarbital (90 mg/kg; i.p.) and the heart was then excised, put into a chilled modified Chapell-Perry 1 (CP1) buffer [100mM KCl, 50mM mM 3-(N-morpholino) propanesulfonic acid(MOPS), 5mM MgSO4•7H2O, 1mM ethylene glycol-bis(2-aminoethylether)-N,N,N',N'-tetraacetic acid(EGTA), and 1mM adenosine 5'-triphosphate disodium(ATP)] at pH 7.4, and then dried with Whatman filter paper. The dried heart was then weighed and placed into an empty beaker on ice. The heart was then minced and transferred to a glass tube with 3mL of Chapell-Perry 2(CP2)[CP1 and 0.2% of Bovine Albumin

Serum(BSA) (#A7030, Sigma Aldrich, Saint Louis, MO)]. The tissue was further minced for 2.5 seconds with a polytron homogenizer at 10,000rpm. The sample was then homogenized with a tight pestle twice using a potter elvehjem homogenizer at 600rpm. A 100µL sample was saved as polytron homogenate (PH) and the rest was centrifuged at 500 x g for 10 min at 4°C. The supernatant was poured into another 15mL centrifuge tube, labeled SSM#1, and the myofibrillar pellet was resuspended in 3mL CP2. This solution was centrifuged at 500 x g for 10 min at 4°C. The supernatant was poured into another 15mL centrifuge tube, labeled SSM#2, and the polytron pellet (PP) was saved for IFM purification. The SSM#1 and SSM#2 supernatants were centrifuged at 3000 x g for 10 min at 4°C. The pellet from SSM#1 was saved for further resuspension as SSM pellet.

The supernatant from the SSM#1 tube was crude cytosol(cCS) and 100µL was saved while the rest was pipetted into two 1mL eppendorf tubes in equal volumes and centrifuged at 22,000 x g for 10min at 4°C. A 0.1µM filter was then used to purify the supernatants and the result was pure cytosol.

The saved polytron pellet was resuspended in 3mL of CP1 along with 5mg/g (wet weight) of trypsin (#T0303, Sigma-Aldrich, Saint Louis, MO). This mixture was incubated in a glass tube, on ice, for 15 min with stirring. After 15 min, 3mL of CP2 was added to stop the effect of trypsin. The sample was homogenized with a tight pestle twice using a potter elvejhem homogenizer at 600rpm. The homogenized sample was then placed in a 15mL tube and centrifuged for 10min at 500 x g at 4°C. The resulting supernatant was poured into another 15mL tube and centrifuged for 10min at 3000 x g at 4°C. The supernatant was then discarded and the pellet was

saved as IFM pellet. Both the SSM pellet and IFM pellet were resuspended in 2mL of KME [100mM KCl, 50mM MOPS, and 0.5mM EGTA] buffer each. They were then centrifuged at 3000 x g for 10 min at 4°C. The resulting supernatants were discarded and the pellets were resuspended in 60µL of KME each. The final volumes for SSM and IFM were measured (Palmer, Tandler, & Hoppel, 1977).

Protein concentrations of SSM, IFM, and purified cytosol were then measured using a Lowry Protein Assay with BSA as the standard and sodium deoxycholate (DOC) [Sigma-Alrdige, Saint Louis, MO] as the detergent.

2.2.2 Measurement of oxidative phosphorylation of SSM and IFM

A Model 782 Oxygen Meter (Strathkelvin Systems, Glasgow, Scotland), glass chamber of a MT200 Mitocell Respirometer (Strathkelvin Instruments, Glasgow, Scotland), and a 1302 Microcathode Oxygen Electrode (Strathkelvin Instruments, Glasgow, Scotland) were used to measure oxygen consumption at 31°C. The glass chamber was filled with 0.5mL of buffer [100mM KCl, 50mM MOPS, 1.0mM EGTA, 5mM KH_2PO_4, and 1mg/mL of defatted BSA]. To measure Complex I respiration, 150µg of SSM was placed in the glass chamber along with 20mM Glutamate and 5mM Malate. To measure State 3 respiration, 10µL of 10mM ADP was added to reach a concentration of 0.2mM ADP and 10µL of 10mM ADP was added once again. State 4 respiration was measured when oxygen consumption slowed as ADP was finished being converted into ATP. Then, 10µL of 100mM ADP was added to reach a final concentration of 2mM ADP. The recording taken at this point was the maximum coupled respiration rate. Finally, 10µL of 10mM of DNP (2,4-dinitrophenol), an uncoupler, was added to measure the maximum uncoupled

respiration rate. The same process was repeated to measure Complex 1 respiration for IFM.

To measure Complex II respiration, 100µg of SSM was used with 20mM Succinate and 2.5µM Rotenone, an inhibitor of Complex 1. State 3, State 4, maximum coupled respiration rate, and maximum uncoupled respiration rate measurements were taken using the same method as above. The same process was used to measure Complex II respiration for IFM.

To measure Complex IV respiration, 50µg of SSM was used with 2.5µM Rotenone. 20µL TMPD and 10µL of 100mM ADP were used as substrates for reducing cytochrome c so Complex IV maximal coupled respiration could be measured (Chen, Moghaddas, Hoppel, & Lesnefsky, 2008).

2.2.3 Measurement of SSM and IFM H_2O_2 production

Hydrogen peroxide production was measured by using Amplex Red (10-acetyl-3, 7-dihydroxyphenoxazine) (A12222, Invitrogen, Carlsbad, CA). In order for hydrogen peroxide to be reduced by horseradish peroxidase (HRP) (Sigma-Aldrich, Saint Louis, MO), Amplex Red's purpose was to be oxidized. This reaction produced resorufin, a fluorescent molecule. An LS55 Fluorescence Spectrophotometer (PerkinElmer Instruments, Waltham, MA) was used to quantitate the amount of resorufin at 31°C with stirring.

Production of H_2O_2 was measured by adding 0.2mg of SSM into 1mL of MMC buffer [150mM KCl, 5mM KH_2PO_4, 1mM EGTA] and 0.95mL of dH_2O. Then, Amplex Red [25 µM] and HRP [0.20 units/mL] was added. To measure H_2O_2 production from Complex I, 10µL of glutamate (6.67mM) and 5µL of malate (3.33mM) were added.

2µL of rotenone (5µM) was then added to block the transfer of electrons from Complex I to Complex II and only measure Complex 1 hydrogen peroxide production (Ross et al., 2013).

The same process was used to measure H_2O_2 production in IFM.

2.2.4 Measurement of SSM and IFM Calcium Retention Capacity

The calcium mediated opening of the mitochondrial pore transition permeability (MPTP) can be measured by Calcium Retention Capacity (CRC). Calcium is gradually added in small concentrations until the MPTP opening results in calcium release from the mitochondria. A LS55 Fluorescence Spectrophotometer (PerkinElmer Instruments, Watham, MA) was used to measure the fluorescence of Calcium-Green 5N (Invitrogen, Carlsbad, CA) at an excitation wavelength of 500nm and an emission wavelength of 530nm.

Firstly, 2mL of CRC buffer [150mM Sucrose, 50mM KCl, 20mM Tris/HCl, 2mM KH_2PO_4, pH 7.4] was mixed with 10µL of 0.5mM Calcium-Green at 31°C with stirring. 0.2mg of SSM was added to the mixture. After one minute, 10µL of $CaCl_2$ was added every 60 seconds until the MPTP opened, indicating the release of calcium. The final measurement was taken as the total concentration of calcium uptake before the release of Ca^{2+} (Chen et al., 2015).

The same process was repeated to measure CRC for IFM.

2.2.5 Measurement of SSM and IFM membrane potential

Tetramethylrhodamine methyl ester (TMRM) is a dye that was used to measure maximum membrane potential and maximum depolarization potential of SSM and IFM. While TMRM is in the cytosol of uncoupled mitochondria, it emits a

fluorescence at a wavelength of 573nm. TMRM that has entered into the mitochondria of depolarized mitochondria shows a fluorescence at a wavelength of 546nm. A LS55 Fluorescence Spectrophotometer (PerkinElmer Instruments, Watham, MA) was used to measure the fluorescence of TMRM and use a ratio between the cytosolic TMRM wavelength and mitochondrial TMRM wavelength to calculate the membrane potential.

In 2mL of respiration buffer [100mM KCl, 50mM MOPS, 1.0mM EGTA, 5mM KH_2PO_4, and 1mg/mL of defatted BSA], 0.2mg of SSM was added along with 10µL of 0.1mM TMRM at 31°C with stirring. Adding 10µL of Glutamate (6.67mM) and 5µL of malate (3.33mM) activated State 2 respiration. State 3 respiration was activated by adding 10µL of 10mM ADP. Adding 2µL of oligomycin caused the membrane potential to be restored as oligomycin inhibits Complex V and protons cannot move down the concentration gradient. Lastly, 10µL of 10mM DNP was added to cause the complete uncoupling of the mitochondria. The difference between the complete uncoupled membrane potential and the State 4 oligomycin membrane potential is the physiologic membrane potential. The difference between State 2 and State 3 respiration is the depolarization potential (Chen, Ross, Hu, & Lesnefsky, 2012).

The same process was used to measure membrane potential and depolarization potential in IFM.

2.2.6. Data Analysis and Statistics

The data is present as mean ± SEM. A one-way ANOVA test was used to compare all results. A two-tailed student's t-test was used to compare differences between the various groups. $P < 0.05$ was considered to be statistically significant.

Chapter 3: Results

3.1. Db/db mice had the highest blood glucose levels out of the four test groups

Before excision of the heart in each mouse, the blood glucose level was checked by glucometer and recorded. As expected, db/db mice, which are known to be hyperglycemic with blood glucose values above 200 mg/dl, showed the highest levels of blood glucose (Keren et al., 2000). Knocking out miR-21, surprisingly, prevented hyperglycemia in the db/db mice as DKO mice had blood glucose levels comparable to C57BL/6J (WT) and miR-21 KO mice, as seen in Figure 3.1.1.

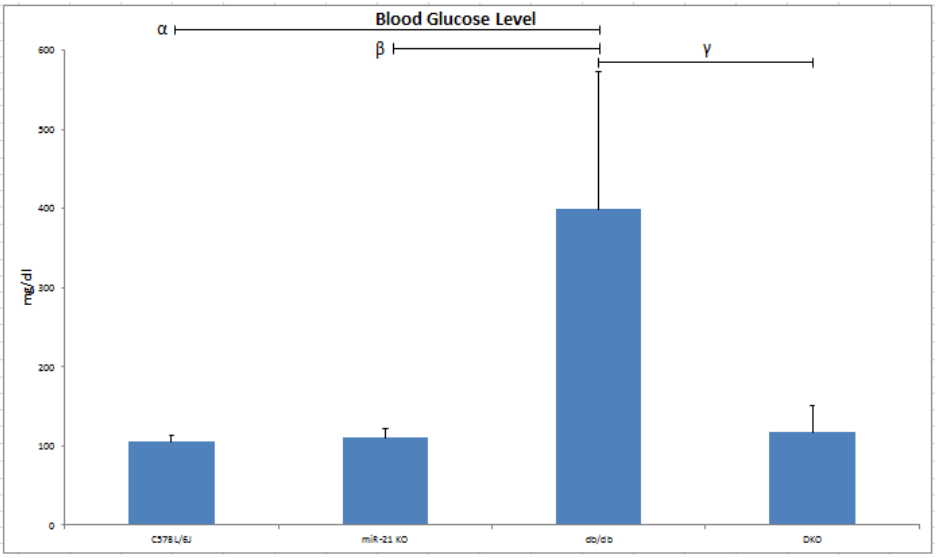

Figure 3.1.1. Db/db mice showed the highest blood glucose levels. The levels are shown in units of mg/dl. The data are presented as both mean ± SEM. A one-way ANOVA test was used to compare all results. $^{\alpha}P < 0.05$ C57BL/6J vs. db/db, $^{\beta}P < 0.05$ miR-21 KO vs. db/db, and $^{\gamma}P < 0.05$ db/db vs. DKO (C57BL/6 n=5, miR-21 KO n=6, db/db n=4, DKO n=6).

3.2. Knocking out miR-21 in diabetic mice augments Complex I function

As described in Methods and Materials, the oxidative phosphorylation activity of Complex I was measured in both SSM and IFM for all four tested groups using glutamate and malate as substrates. For state 3 respiration, maximum coupled respiration, and maximum uncoupled respiration, DKO SSM and IFM had higher oxygen consumption rates than db/db SSM and IFM IFM, as shown in Figures 3.2.2, 3.2.3, 3.2.5, 3.2.6, 3.2.8, and 3.2.9.

Although few results were statistically insignificant, the overall trend in all the measured variables was that db/db SSM and IFM showed lower rates of oxygen consumption than C57BL/6J mice, as shown in Figures 3.2.2, 3.2.3, 3.2.5, 3.2.6, 3.2.8, and 3.2.9.

While the trend in WT, db/db, and DKO mice was that IFM showed higher oxygen consumption rates than SSM in the measured variables, the results were only statistically significant for DKO mice in maximum coupled respiration and in db/db mice as well as DKO mice in maximum uncoupled respiration, as seen in Figures 3.2.4 and 3.2.7.

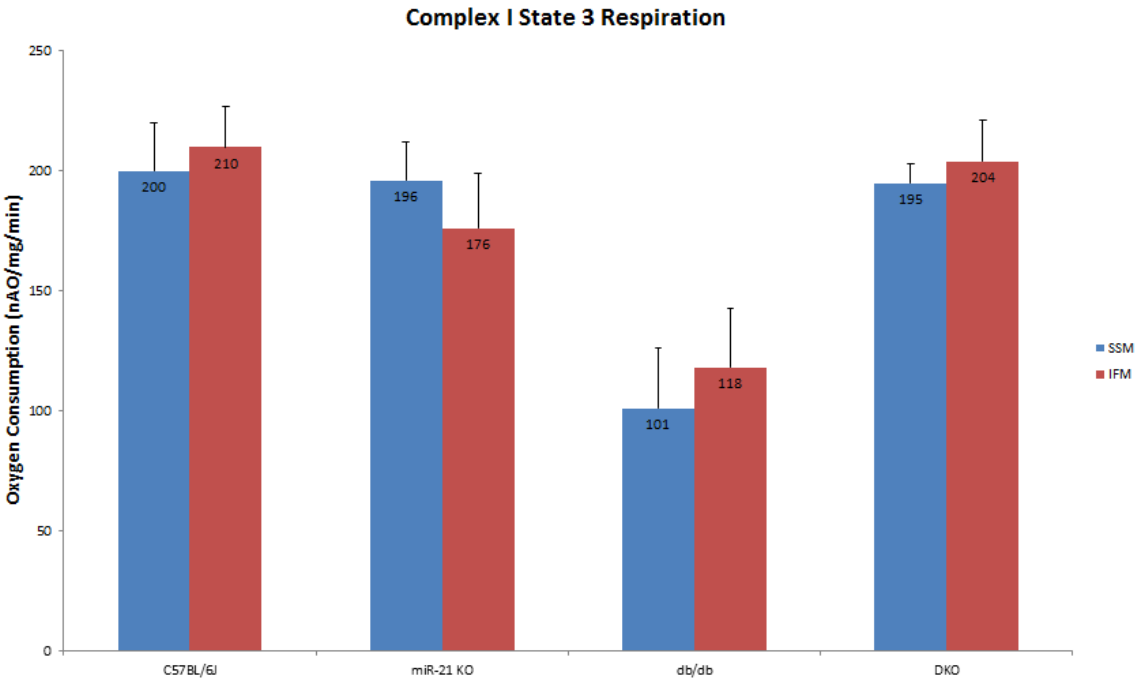

Figure 3.2.1. There are no significant differences between SSM and IFM oxygen consumption in each of the test groups. Complex I State 3 respiration rates were measured using the procedure described in Methods and Materials. The unit of measurement was nanoatoms of atomic oxygen per mg of mitochondria per minute (nAO/mg/min). The data are presented as the mean ± SEM. A one-way ANOVA test was performed to compare the results. *P < 0.05 (C57BL/6 n=5, miR-21 KO n=6, db/db n=4, DKO n=6).

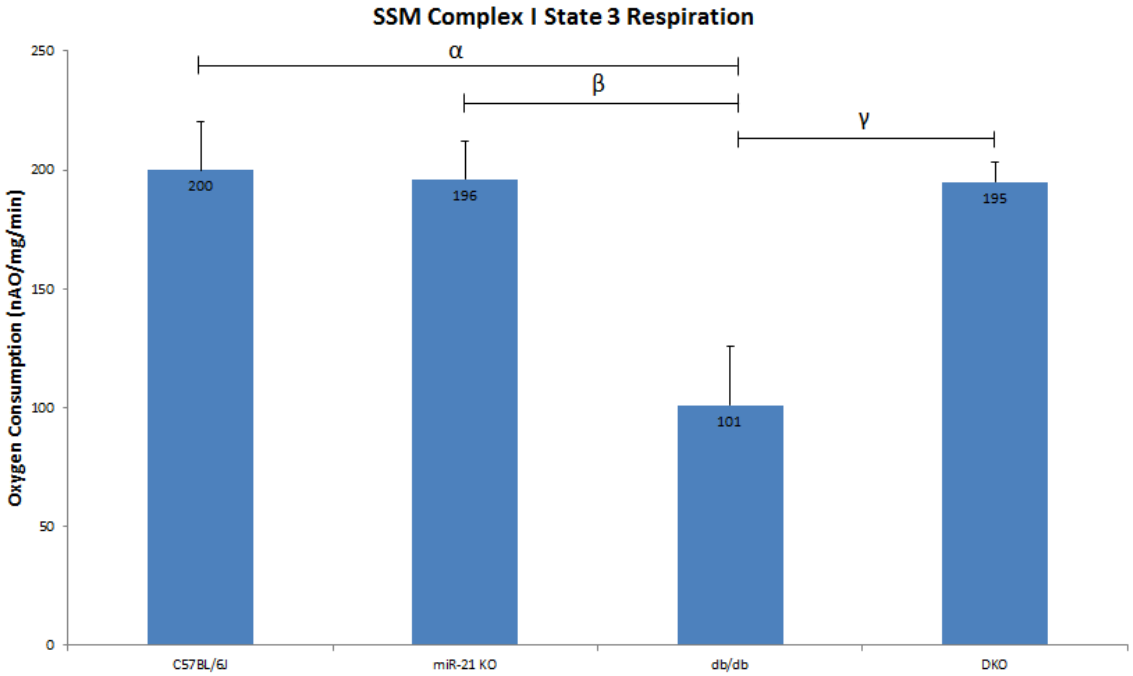

Figure. 3.2.2. Db/db mice have the lowest oxygen consumption rates. Complex I State 3 respiration rates were measured using the procedure described in Methods and Materials. The unit of measurement was nanoatoms of atomic oxygen per mg of mitochondria per minute (nAO/mg/min). The data are presented as the mean ± SEM. A one-way ANOVA test was performed to compare the results. $^{\alpha}P < 0.05$ C57BL/6J vs. db/db, $^{\beta}P < 0.05$ miR-21 KO vs. db/db, and $^{\gamma}P < 0.05$ db/db vs. DKO (C57BL/6J n=5, miR-21 KO n=6, db/db n=4, DKO n=6).

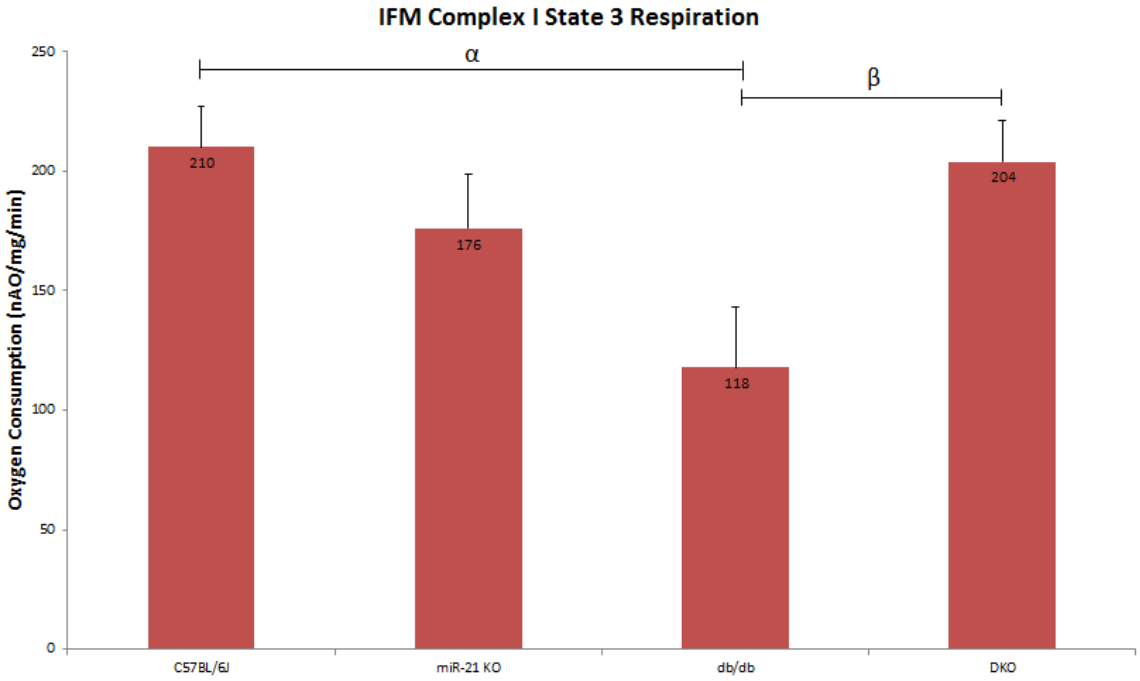

Figure. 3.2.3. Db/db IFM have lower oxygen consumption rates than WT and DKO mice. Complex I State 3 respiration rates were measured using the procedure described in Methods and Materials. The unit of measurement was nanoatoms of atomic oxygen per mg of mitochondria per minute (nAO/mg/min). The data are presented as the mean ± SEM. A one-way ANOVA test was performed to compare the results. $^{\alpha}P < 0.05$ C57BL/6J vs. db/db and $^{\beta}P < 0.05$ db/db vs. DKO (C57BL/6J n=5, miR-21 KO n=6, db/db n=4, DKO n=6).

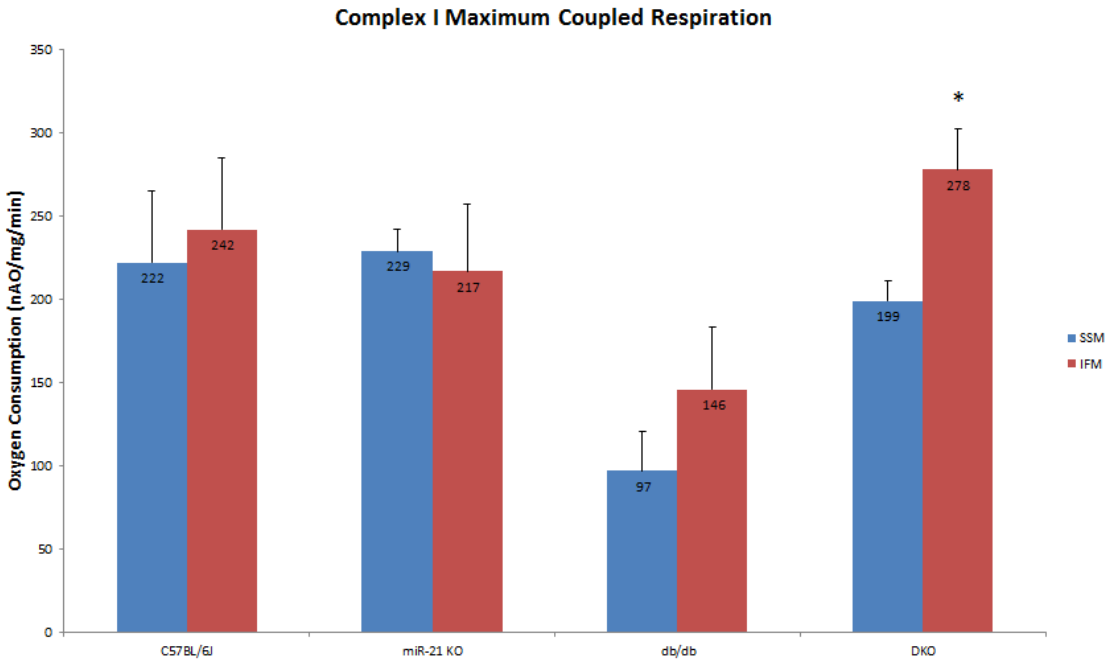

Figure 3.2.4. The rate of oxygen consumption is higher in IFM than SSM for only the DKO group. Complex I maximum coupled respiration rates were measured using the procedure described in Methods and Materials. The unit of measurement was nanoatoms of atomic oxygen per mg of mitochondria per minute (nAO/mg/min). The data are presented as the mean ± SEM. A one-way ANOVA test was performed to compare the results. *P < 0.05 for DKO IFM vs. DKO SSM (C57BL/6J n=5, miR-21 KO n=6, db/db n=4, DKO n=6).

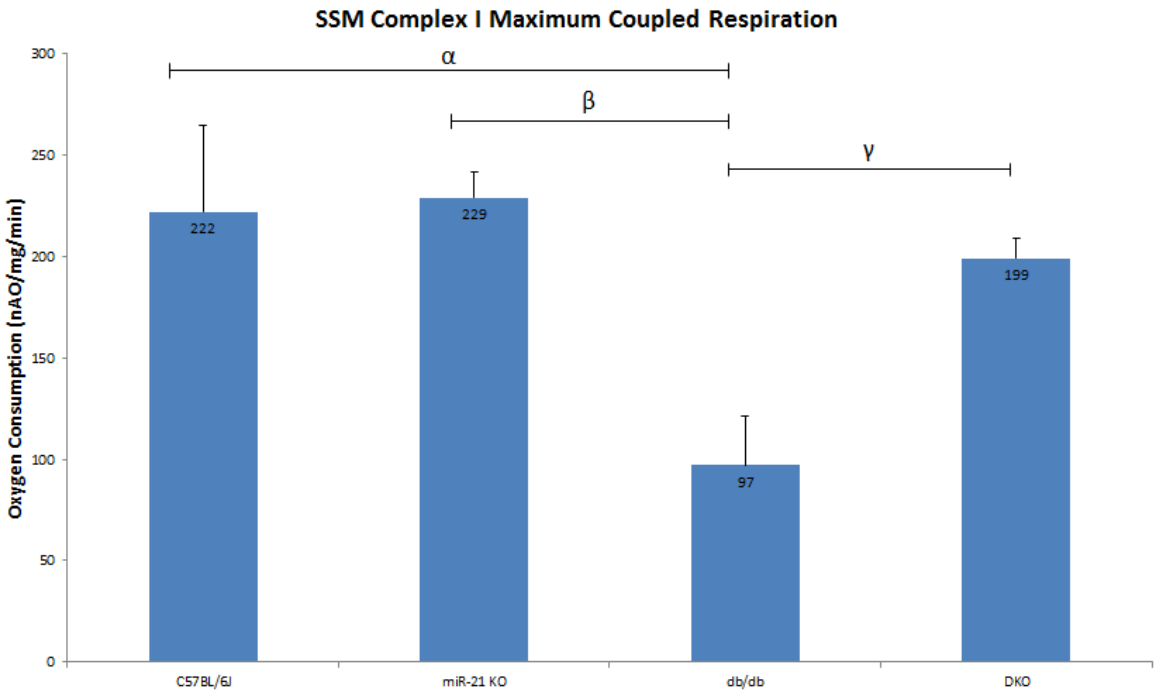

Figure. 3.2.5. Db/db mice have the lowest oxygen consumption rates among the test groups. Complex I maximum coupled respiration rates were measured using the procedure described in Methods and Materials. The unit of measurement was nanoatoms of atomic oxygen per mg of mitochondria per minute (nAO/mg/min). The data are presented as the mean ± SEM. A one-way ANOVA test was performed to compare the results. $^{\alpha}P < 0.05$ C57BL/6J vs. db/db, $^{\beta}P < 0.05$ miR-21 KO vs. db/db, and $^{\gamma}P < 0.05$ db/db vs. DKO, (C57BL/6J n=5, miR-21 KO n=6, db/db n=4, DKO n=6).

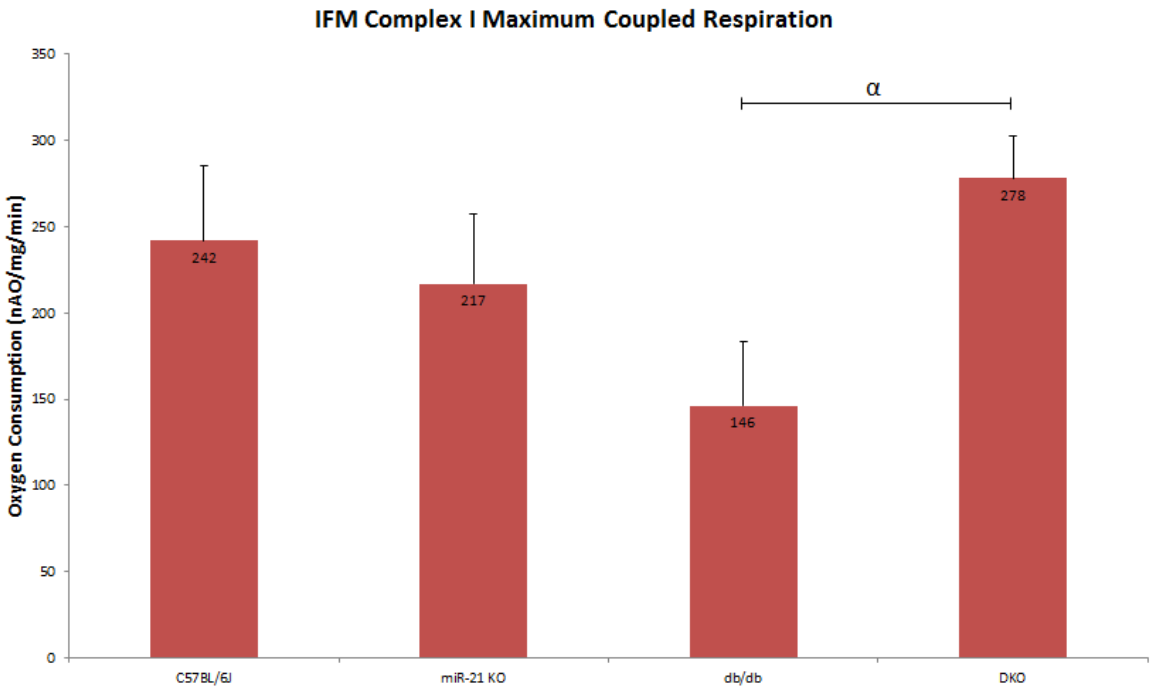

Figure. 3.2.6. The oxygen consumption rates for db/db IFM are lower than DKO IFM. Complex I maximum coupled respiration rates were measured using the procedure described in Methods and Materials. The unit of measurement was nanoatoms of atomic oxygen per mg of mitochondria per minute (nAO/mg/min). The data are presented as the mean ± SEM. A one-way ANOVA test was performed to compare the results. $^{\alpha}P < 0.05$ db/db vs. DKO (C57BL/6J n=5, miR-21 KO n=6, db/db n=4, DKO n=6).

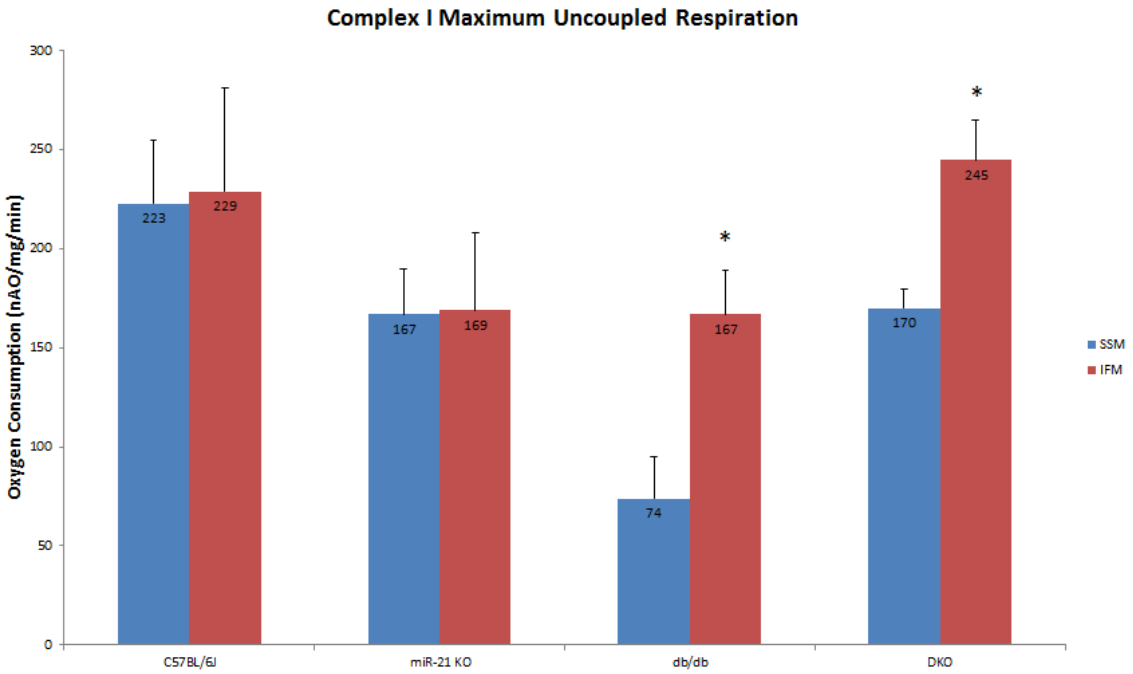

Figure 3.2.7. The rate of oxygen consumption is higher in IFM than SSM for the db/db and DKO groups. Complex I maximum uncoupled respiration rates were measured using the procedure described in Methods and Materials. The unit of measurement was nanoatoms of atomic oxygen per mg of mitochondria per minute (nAO/mg/min). The data are presented as the mean ± SEM. A one-way ANOVA test was performed to compare the results. *P < 0.05 for db/db SSM vs. db/db IFM and DKO SSM vs. DKO IFM (C57BL/6J n=5, miR-21 KO n=6, db/db n=4, DKO n=6).

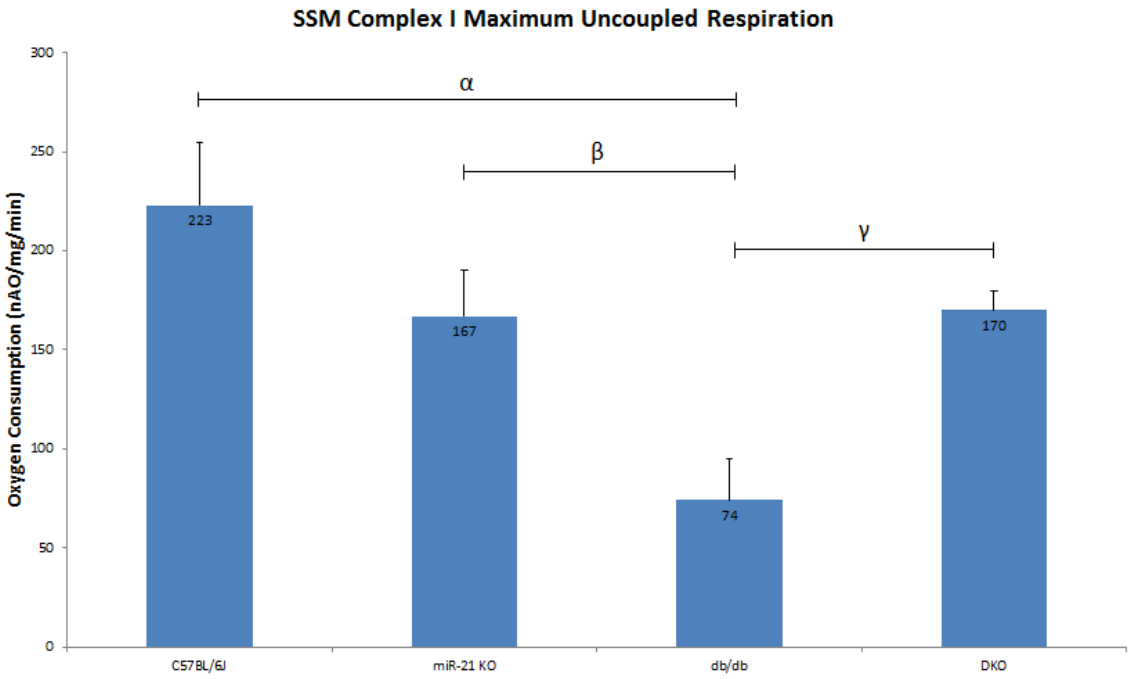

Figure. 3.2.8. Db/db SSM have the lowest oxygen consumption rates. Complex I maximum uncoupled respiration rates were measured using the procedure described in Methods and Materials. The unit of measurement was nanoatoms of atomic oxygen per mg of mitochondria per minute (nAO/mg/min). The data are presented as the mean ± SEM. A one-way ANOVA test was performed to compare the results. $^{\alpha}P < 0.05$ C57BL/6J vs. db/db, $^{\beta}P < 0.05$ miR-21 KO vs. db/db, and $^{\gamma}P < 0.05$ db/db vs. DKO (C57BL/6J n=5, miR-21 KO n=6, db/db n=4, DKO n=6).

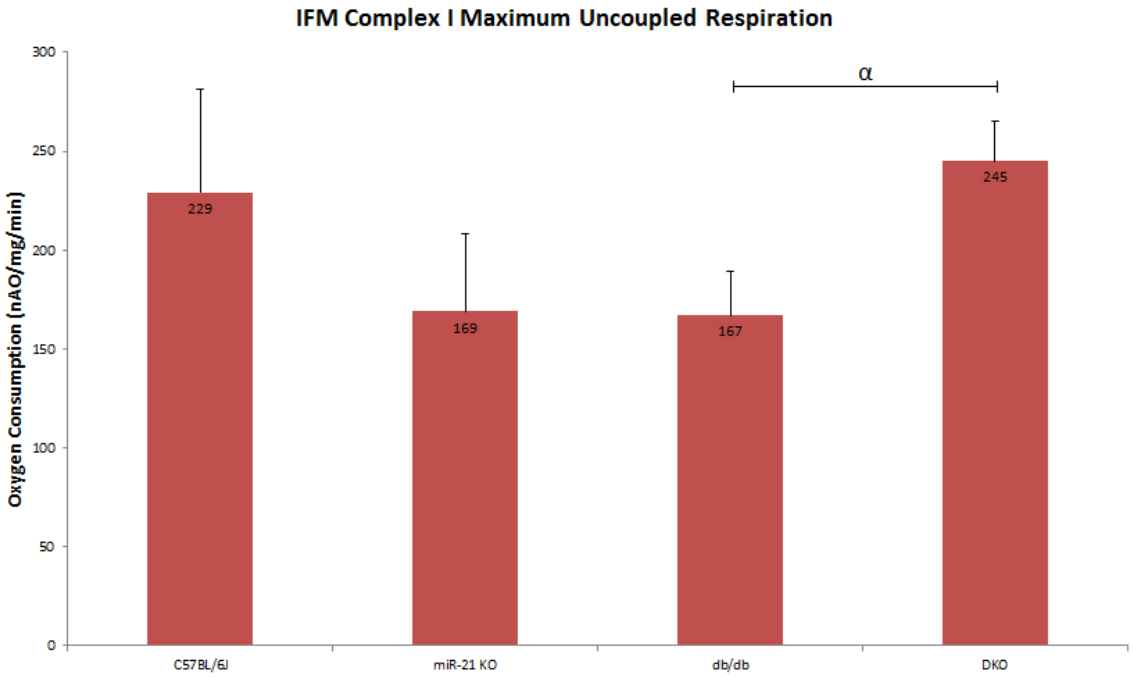

Figure. 3.2.9. The oxygen consumption rates for db/db IFM are lower than DKO IFM. Complex I maximum uncoupled respiration rates were measured using the procedure described in Methods and Materials. The unit of measurement was nanoatoms of atomic oxygen per mg of mitochondria per minute (nAO/mg/min). The data are presented as the mean ± SEM. A one-way ANOVA test was performed to compare the results. $^{\alpha}P < 0.05$ db/db vs. DKO (C57BL/6J n=5, miR-21 KO n=6, db/db n=4, DKO n=6)..

3.3. In Complex II, knocking out miR-21 from diabetic mice generally increases function of both SSM and IFM

Complex II function was measured in SSM and IFM for all four test groups, using succinate and rotenone as the substrates, by the procedure described in the Methods and Materials section. In Complex II state 3 respiration, DKO SSM had higher rates of oxygen consumption than db/db SSM. The same result was true for DKO IFM compared to db/db IFM. DKO SSM and IFM had higher rates than db/db SSM and IFM in maximum coupled respiration as well, although the results were not significant. DKO SSM had higher rates of maximum uncoupled respiration than db/db SSM and the same was true for IFM, but the difference was not significant.

MiR-21 KO SSM showed an increase in state 3 respiration compared to WT SSM but there was no significant difference in IFM. MiR-21 KO SSM also showed a significant increase in maximum coupled respiration and an insignificant increase in maximum uncoupled respiration compared to WT SSM. The changes in IFM were not significant.

Db/db mice also generally showed a reduction in Complex II function compared when compared to miR-21 KO mice and C57BL/6J mice. Even though some results were not significant, the overall trend was still present.

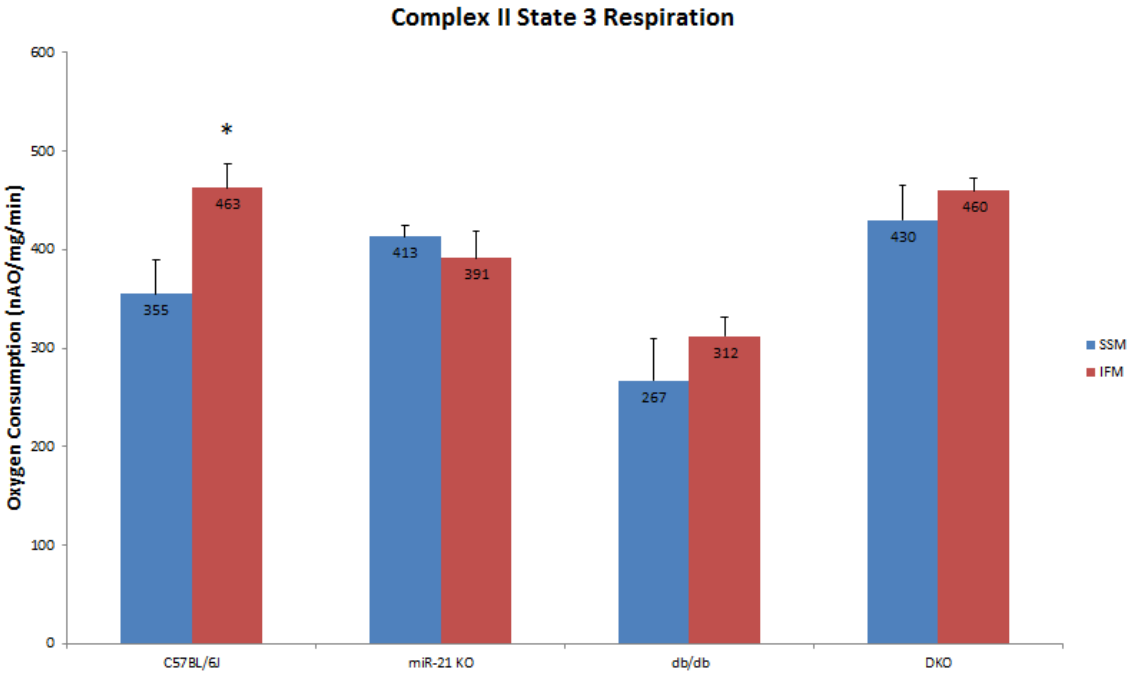

Figure 3.3.1. C57BL/6J IFM had higher oxygen consumption rates than SSM. Complex II State 3 respiration rates were measured using the procedure described in Methods and Materials. The unit of measurement was nanoatoms of atomic oxygen per mg of mitochondria per minute (nAO/mg/min). The data are presented as the mean ± SEM. A one-way ANOVA test was performed to compare the results. $^{\alpha}P < 0.05$ C57BL/6J SSM vs. C57BL/6J IFM (C57BL/6J n=5, miR-21 KO n=6, db/db n=4, DKO n=6).

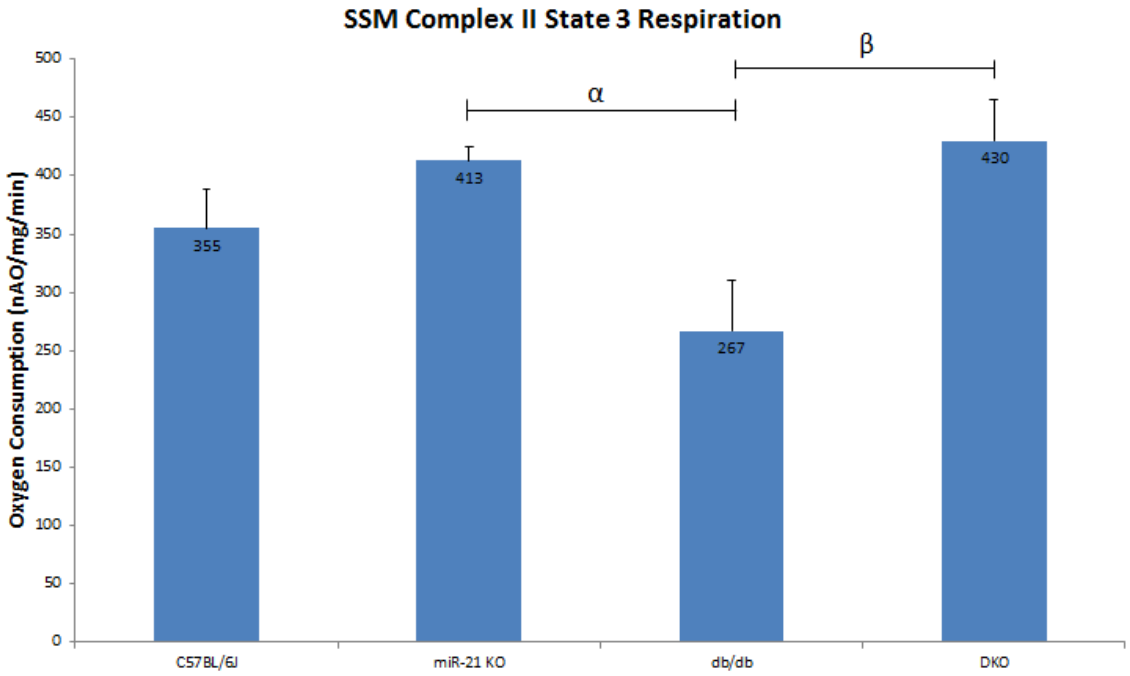

Figure 3.3.2. Db/db SSM have lower oxygen consumption rates than miR-21 KO and DKO SSM. Complex II State 3 respiration rates were measured using the procedure described in Methods and Materials. The unit of measurement was nanoatoms of atomic oxygen per mg of mitochondria per minute (nAO/mg/min). The data are presented as the mean ± SEM. A one-way ANOVA test was performed to compare the results. $^{\alpha}P < 0.05$ miR-21 KO vs. db/db, $^{\beta}P < 0.05$ db/db vs. DKO (C57BL/6J n=5, miR-21 KO n=6, db/db n=4, DKO n=6).

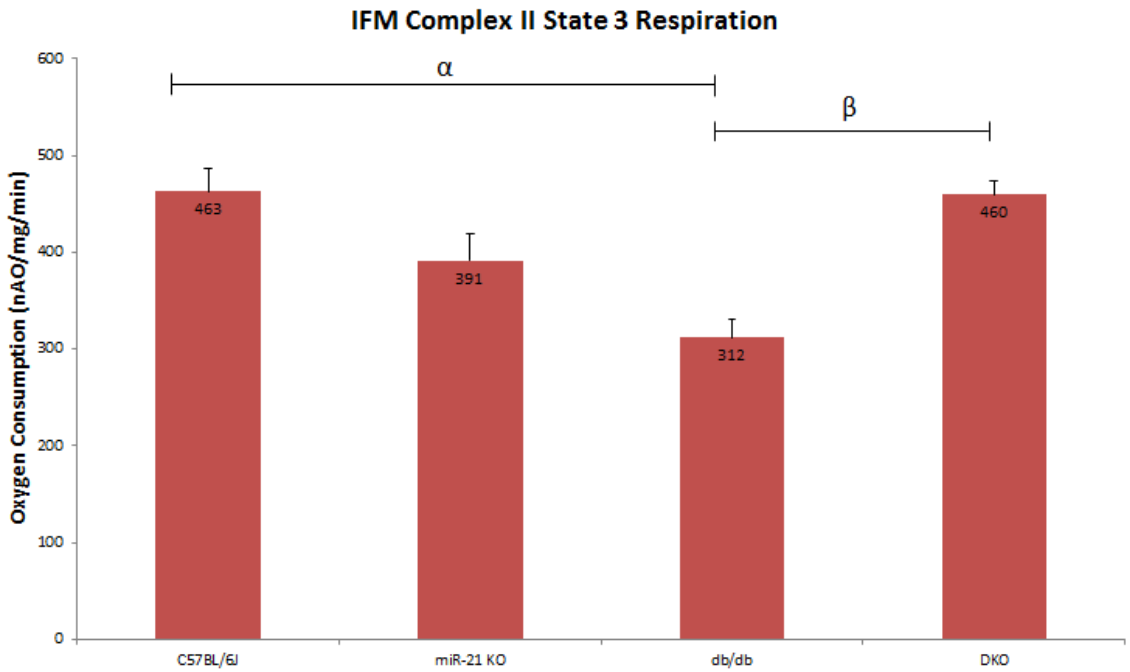

Figure. 3.3.3. The oxygen consumption rate for db/db IFM is lower than C57BL/6J IFM and DKO IFM. Complex II State 3 respiration rates were measured using the procedure described in Methods and Materials. The unit of measurement was nanoatoms of atomic oxygen per mg of mitochondria per minute (nAO/mg/min). The data are presented as the mean ± SEM. A one-way ANOVA test was performed to compare the results. $^{\alpha}P < 0.05$ C57BL/6J vs. db/db and $^{\beta}P < 0.05$ db/db vs. DKO (C57BL/6J n=5, miR-21 KO n=6, db/db n=4, DKO n=6).

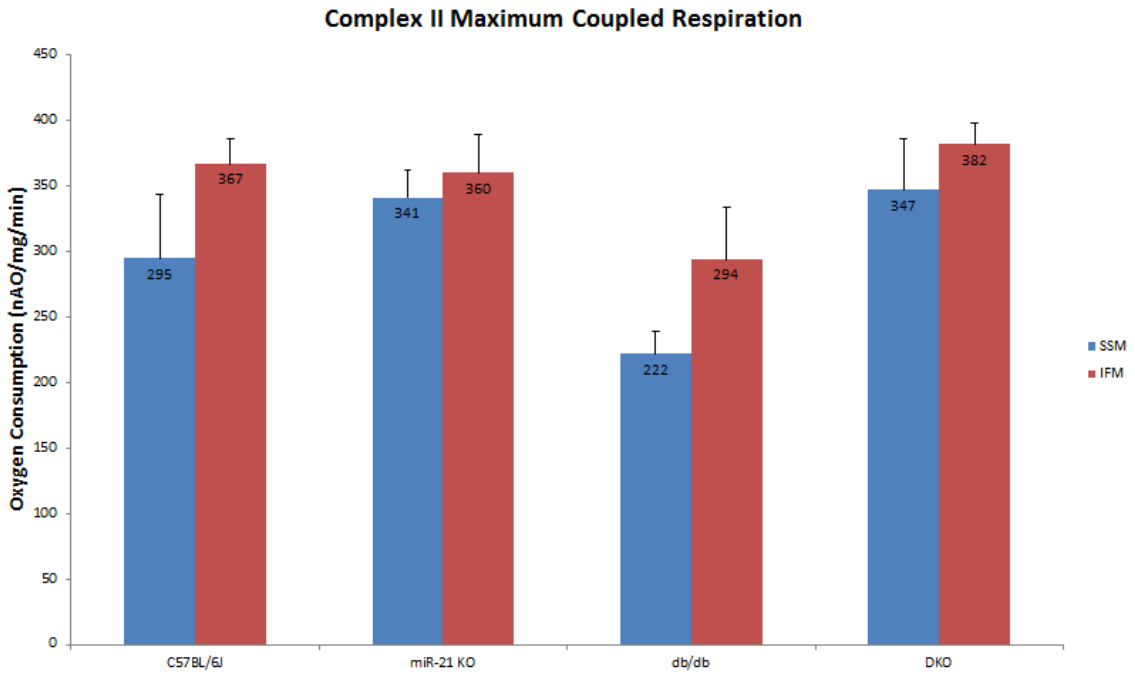

Figure 3.3.4. There are no significant differences between SSM and IFM oxygen consumption rates in the test groups. Complex II maximum coupled respiration rates were measured using the procedure described in Methods and Materials. The unit of measurement was nanoatoms of atomic oxygen per mg of mitochondria per minute (nAO/mg/min). The data are presented as the mean ± SEM. A one-way ANOVA test was performed to compare the results. $P < 0.05$ (C57BL/6J n=5, miR-21 KO n=6, db/db n=4, DKO n=6).

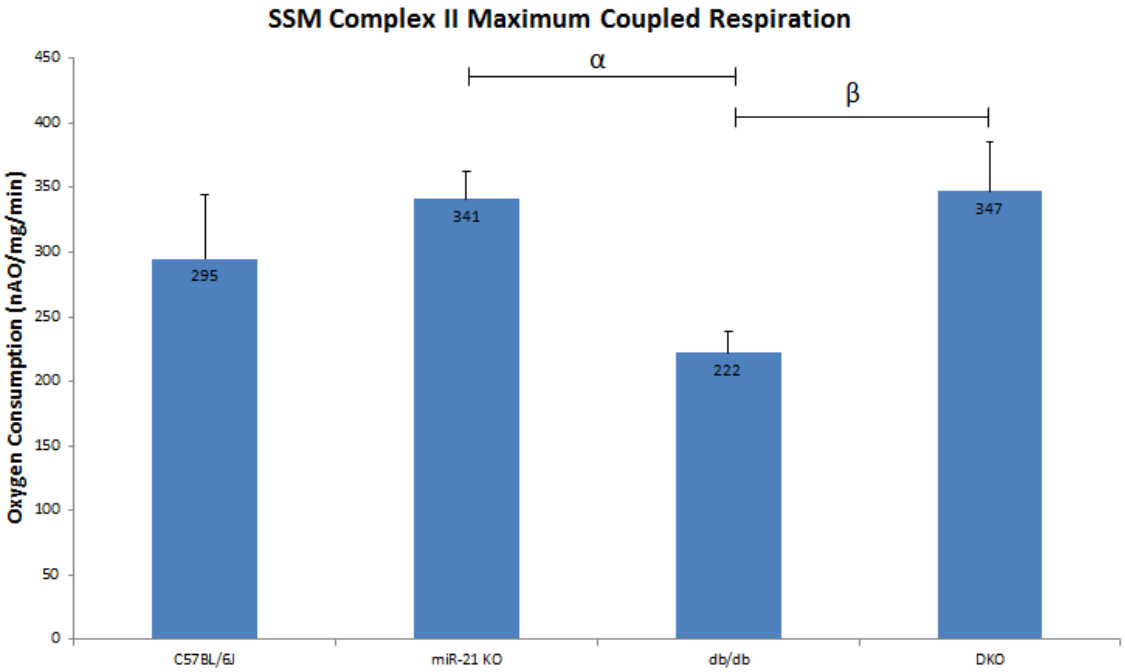

Figure 3.3.5. Db/db SSM has lower rates than miR-21 KO and DKO SSM.

Complex II maximum coupled respiration rates were measured using the procedure described in Methods and Materials. The unit of measurement was nanoatoms of atomic oxygen per mg of mitochondria per minute (nAO/mg/min). The data are presented as the mean ± SEM. A one-way ANOVA test was performed to compare the results. $^{\alpha}P < 0.05$ miR-21 KO vs. db/db and $^{\beta}P < 0.05$ db/db vs. DKO (C57BL/6J n=5, miR-21 KO n=6, db/db n=4, DKO n=6).

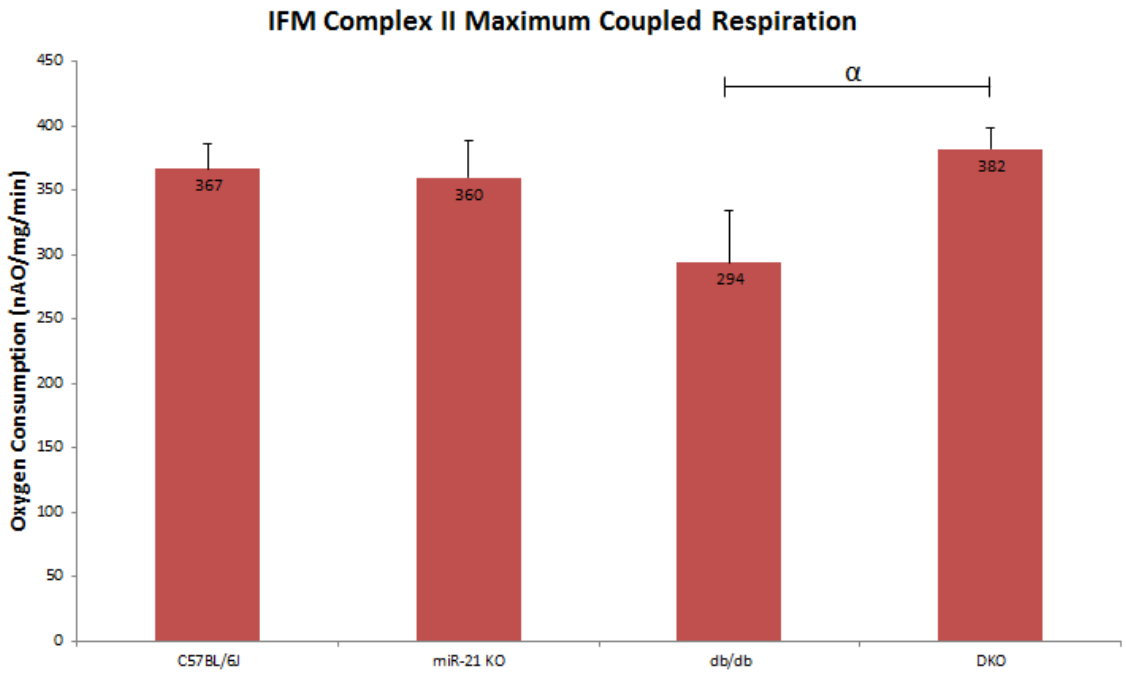

Figure. 3.3.6. Db/db IFM had lower rates than DKO IFM. Complex II maximum coupled respiration rates were measured using the procedure described in Methods and Materials. The unit of measurement was nanoatoms of atomic oxygen per mg of mitochondria per minute (nAO/mg/min). The data are presented as the mean ± SEM. A one-way ANOVA test was performed to compare the results. $^{\alpha}P < 0.05$ db/db vs. DKO (C57BL/6J n=5, miR-21 KO n=6, db/db n=4, DKO n=6).

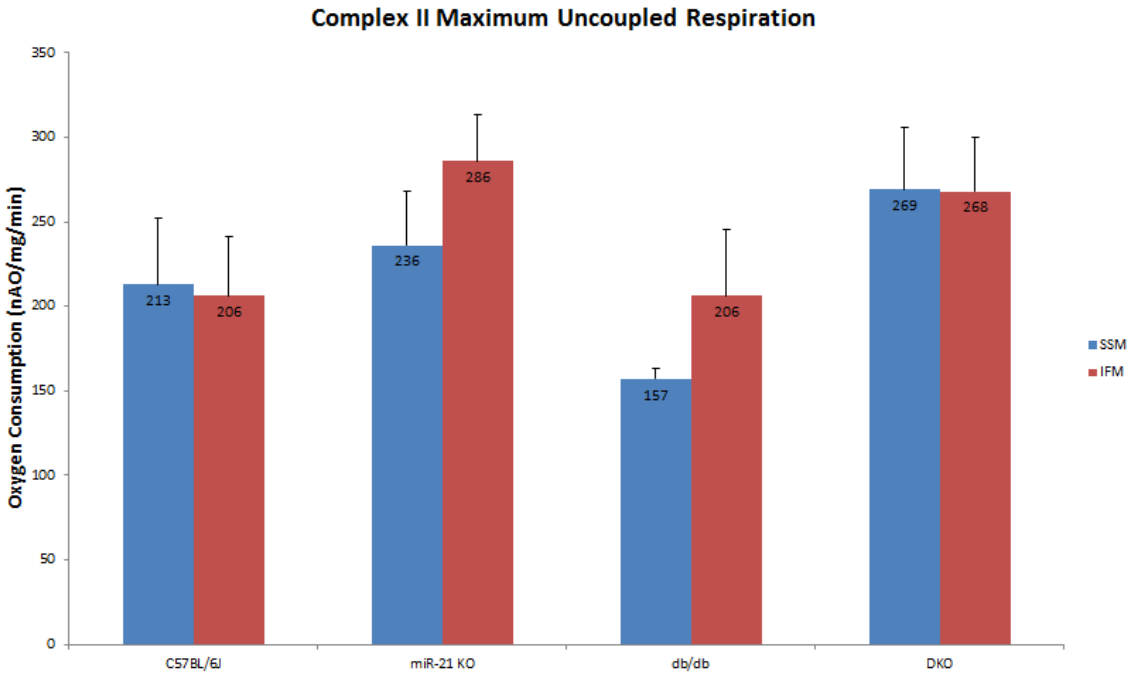

Figure 3.3.7. The rates of oxygen consumption in IFM and SSM were not significantly different within each group. Complex II maximum uncoupled respiration rates were measured using the procedure described in Methods and Materials. The unit of measurement was nanoatoms of atomic oxygen per mg of mitochondria per minute (nAO/mg/min). The data are presented as the mean ± SEM. A one-way ANOVA test was performed to compare the results. $P < 0.05$ (C57BL/6J n=5, miR-21 KO n=6, db/db n=4, DKO n=6).

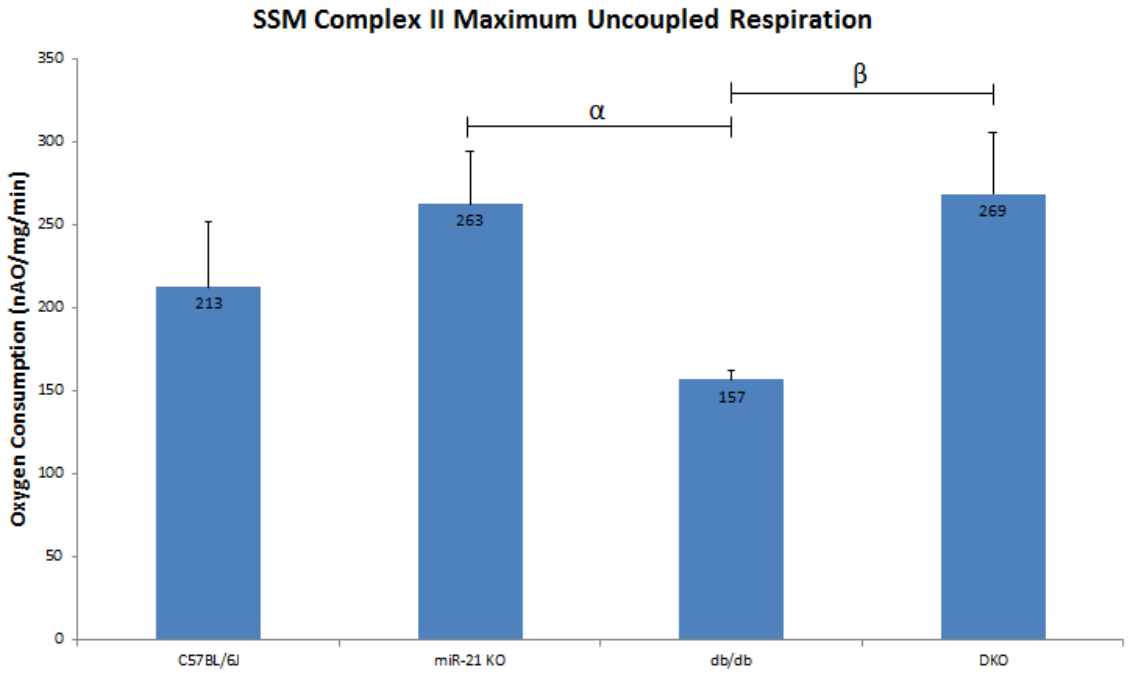

Figure 3.3.8. Db/db SSM has lower rates than miR-21 KO SSM and DKO SSM. Complex II maximum uncoupled respiration rates were measured using the procedure described in Methods and Materials. The unit of measurement was nanoatoms of atomic oxygen per mg of mitochondria per minute (nAO/mg/min). The data are presented as the mean ± SEM. A one-way ANOVA test was performed to compare the results. $^{\alpha}P < 0.05$ miR-21 KO vs. db/db and $^{\beta}P < 0.05$ db/db vs. DKO (C57BL/6J n=5, miR-21 KO n=6, db/db n=4, DKO n=6).

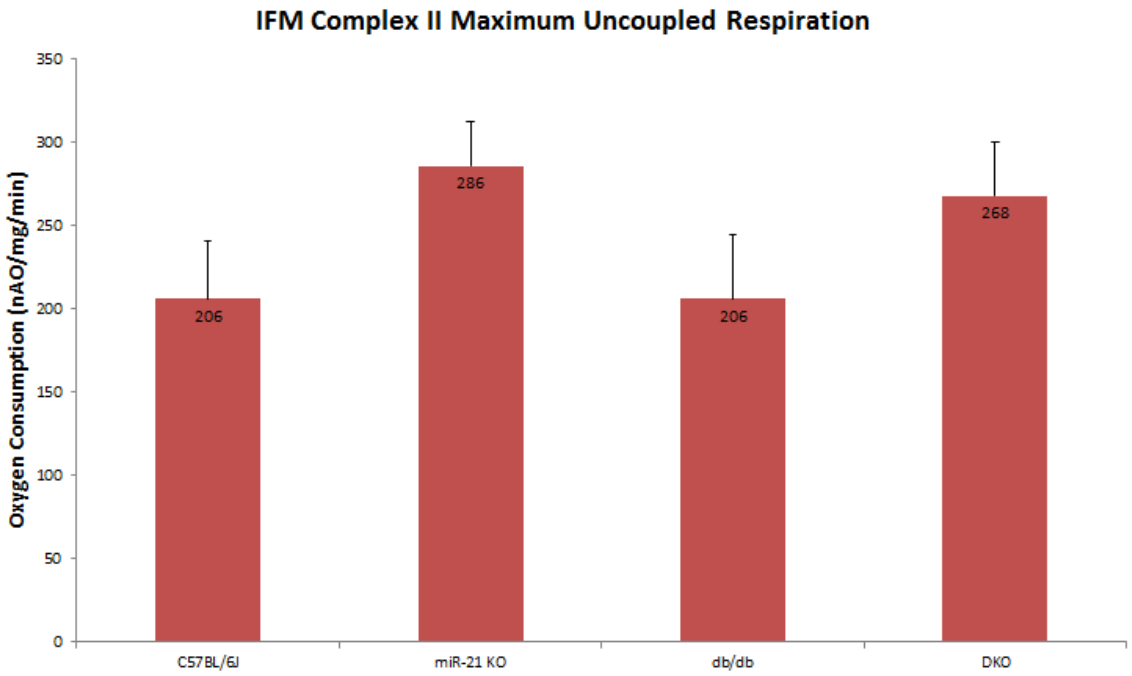

Figure. 3.3.9. The oxygen consumption rates for IFM were not significantly different among the four groups. Complex II maximum uncoupled respiration rates were measured using the procedure described in Methods and Materials. The unit of measurement was nanoatoms of atomic oxygen per mg of mitochondria per minute (nAO/mg/min). The data are presented as the mean ± SEM. A one-way ANOVA test was performed to compare the results. $P < 0.05$ for comparison (C57BL/6J n=5, miR-21 KO n=6, db/db n=4, DKO n=6).

3.4. Knocking out miR-21 does not have a major effect on Complex IV coupled respiration rates

As described in Methods and Materials, the maximum coupled respiration rates of Complex IV were measured in both SSM and IFM for all four tested groups. No significant differences were seen when comparing SSM oxygen consumption rates to IFM oxygen consumption rates. No significant differences were seen when comparing each SSM group to the other SSM test groups. Even though some results were not significant, the overall trend was that DKO IFM showed higher oxygen consumption rates than WT IFM, miR-21 KO IFM, and db/db IFM, as seen in Figure 3.4.1.

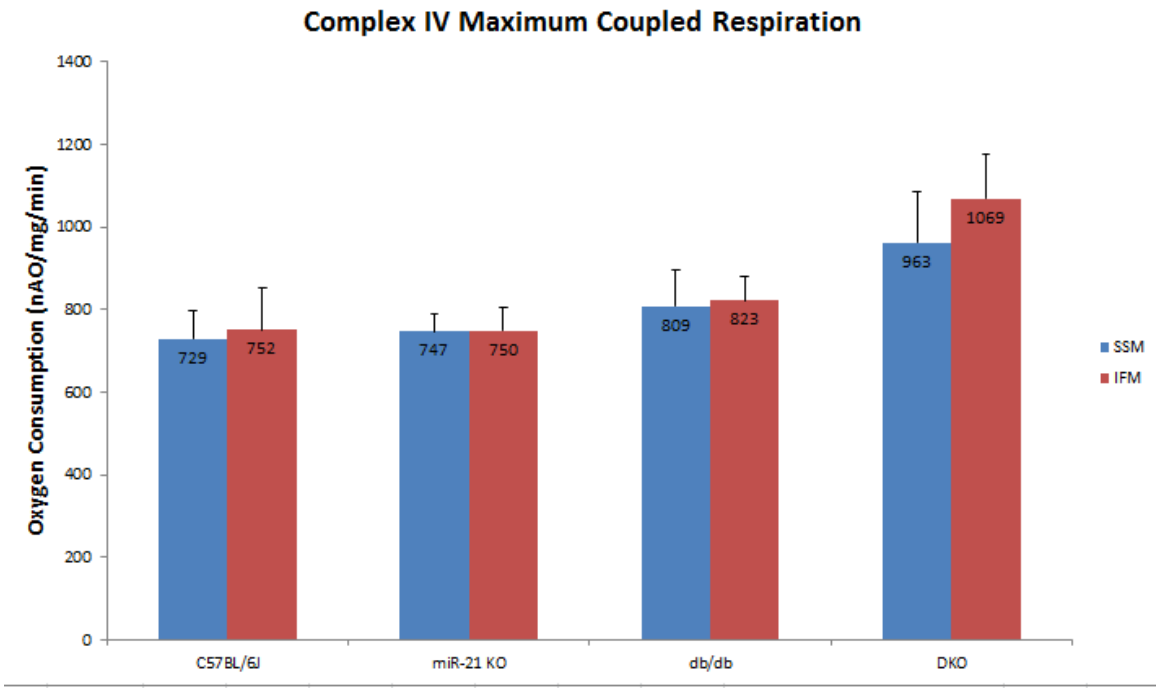

Figure 3.4.1. There were no significant differences between SSM and IFM and also between each of the test groups. Complex IV maximum coupled respiration rates were measured using the procedure described in Methods and Materials. The unit of measurement was nanoatoms of atomic oxygen per mg of mitochondria per minute (nAO/mg/min). The data are presented as the mean ± SEM. A one-way ANOVA test was performed to compare the results. $P < 0.05$ for all comparisons (C57BL/6J n=5, miR-21 KO n=6, db/db n=4, DKO n=6).

3.5. db/db IFM show greater ability for handling calcium than db/db SSM

Calcium retention capacity, as described in Methods and Materials, was used to measure the calcium handling ability of SSM and IFM for each of the four tested groups and to provide a marker for the sensitivity of each group to MPTP opening. In the db/db group, IFM were able to retain more calcium than SSM, as seen in Figure 3.5.1.

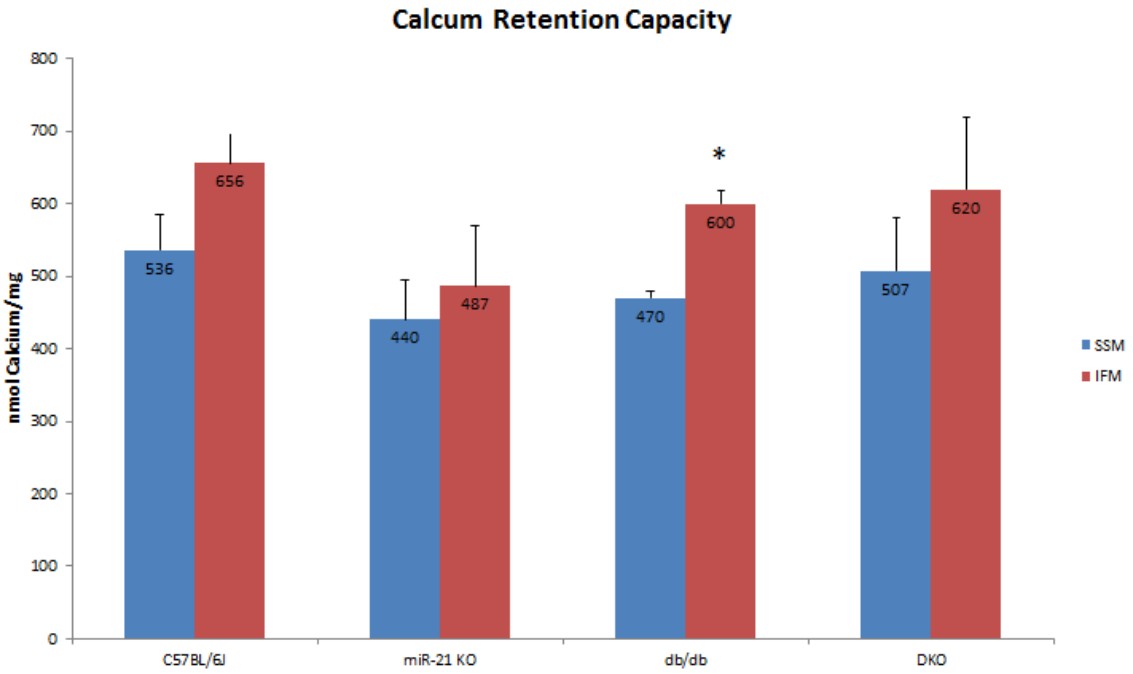

Figure 3.5.1. The calcium retention for IFM is higher than SSM only in the db/db group. As described in Methods and Materials, the calcium retention capacity was measured in SSM and IFM for each of the four groups. The unit of measurement was nanomolars of Calcium per mg of mitochondria. The data is shown as mean ± SEM. A one way ANOVA was performed to compare the results. *P < 0.05 for db/db SSM vs. db/db IFM (C57BL/6J n=5, miR-21 KO n=6, db/db n=4, DKO n=6).

3.6. The membrane depolarization potential was higher in DKO SSM and IFM compared to most other groups

Tetramethylrhodamine methyl ester (TMRM) is a dye that was used to measure membrane depolarization potential of SSM and IFM in each of the four groups, as described in Methods and Materials.

DKO SSM showed the highest depolarization potential compared to the miR-21 KO and db/db groups while DKO IFM showed higher potentials than all three other groups, as seen in Figures 3.6.2 and 3.6.3.

IFM showed lower depolarization potentials compared to SSM in the C57BL/6J and db/db groups, as shown in Figure 3.6.1.

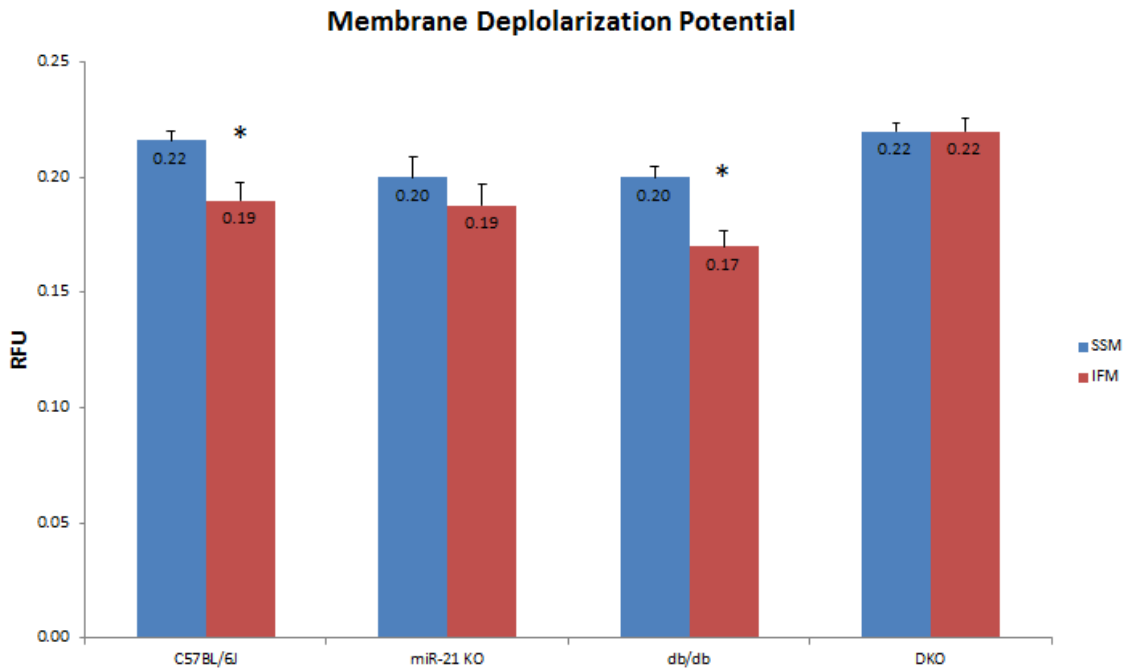

Figure 3.6.1. SSM showed higher membrane depolarization potentials in the WT and db/db groups. A TMRM dye was used to measure membrane depolarization potential of SSM and IFM in each of the four test groups according to the procedure described in Methods and Materials. The depolarization potential was measured in units of RFU (Relative Fluorescence Units). The data is shown as mean ± SEM. A one way ANOVA was performed to compare the results. $^{*}P < 0.05$ C57BL/6J IFM vs. C57BL/6J IFM and db/db SSM vs. db/db IFM (C57BL/6J n=5, miR-21 KO n=6, db/db n=4, DKO n=6).

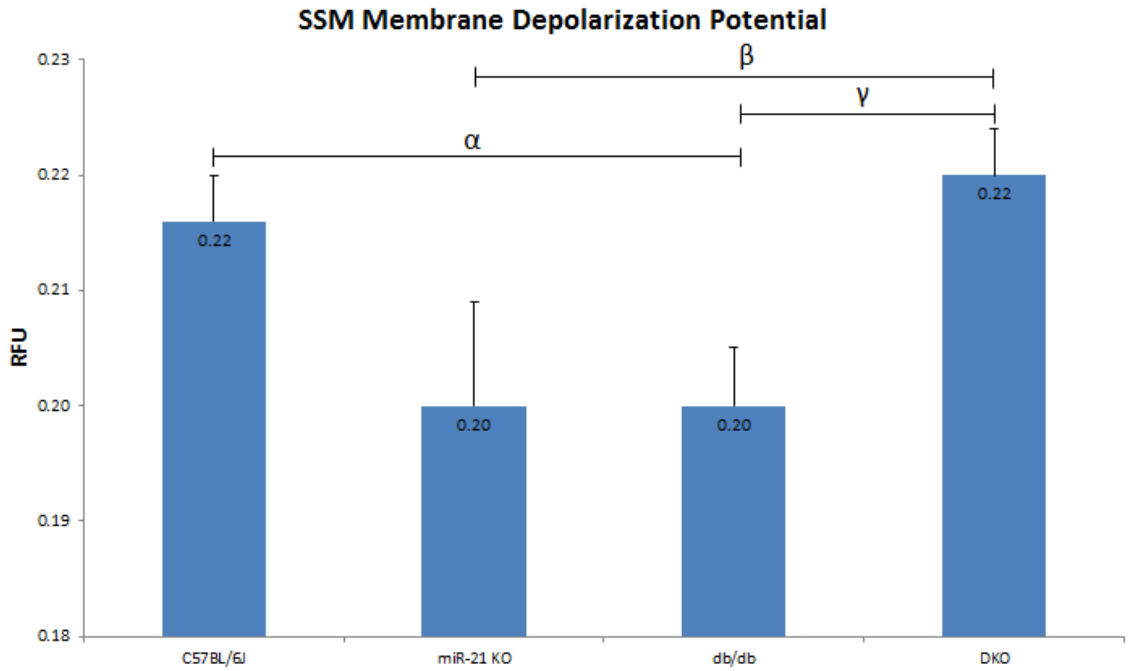

Figure 3.6.2. DKO SSM had a higher membrane depolarization potential than miR-21 KO and db/db SSM while WT SSM depolarization potential was also higher than db/db SSM. A TMRM dye was used to measure membrane depolarization potential of SSM in each of the four test groups according to the procedure described in Methods and Materials. The depolarization potential was measured in units of RFU (Relative Fluorescence Units). The data is shown as mean ± SEM. A one way ANOVA was performed to compare the results. $^{\alpha}P < 0.05$ C57BL/6J vs. db/db, $^{\beta}P < 0.05$ miR-21 KO vs. DKO, and $^{\gamma}P < 0.05$ db/db vs. DKO (C57BL/6J n=5, miR-21 KO n=6, db/db n=4, DKO n=6).

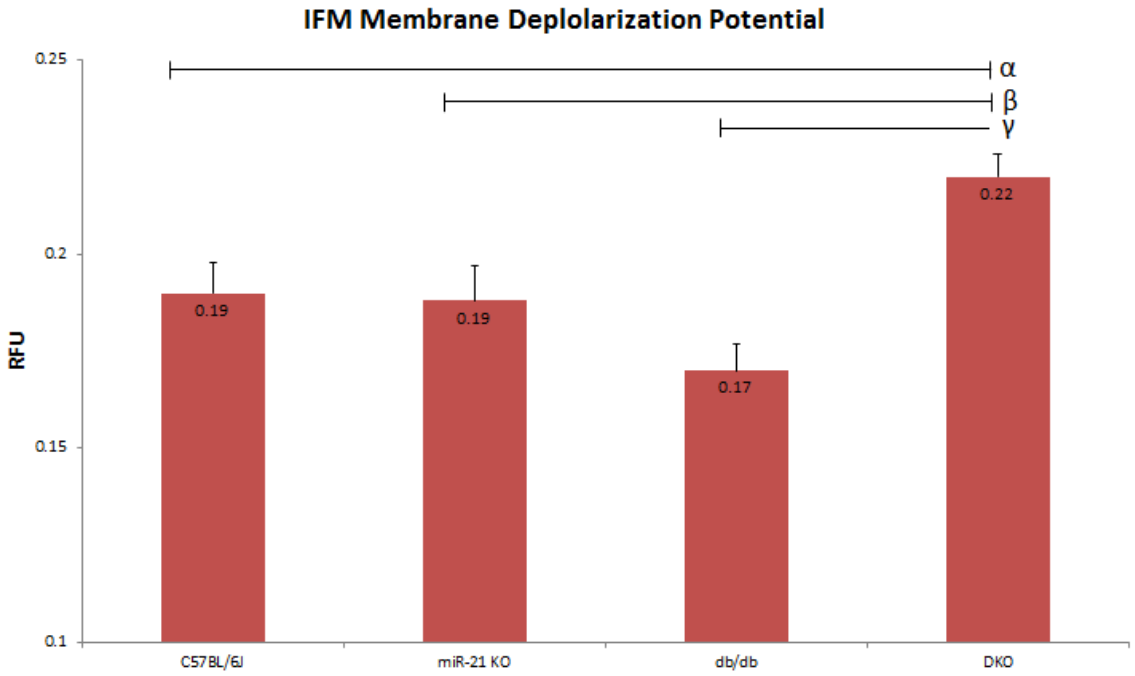

Figure 3.6.3. DKO IFM had a higher membrane depolarization potential than the other test groups. A TMRM dye was used to measure membrane depolarization potential of SSM in each of the four test groups according to the procedure described in Methods and Materials. The depolarization potential was measured in units of RFU (Relative Fluorescence Units). The data is shown as mean ± SEM. A one way ANOVA was performed to compare the results. $^{\alpha}P < 0.05$ C57BL/6J vs. DKO, $^{\beta}P < 0.05$ miR-21 KO vs. DKO, and $^{\gamma}P < 0.05$ db/db vs. DKO (C57BL/6J n=5, miR-21 KO n=6, db/db n=4, DKO n=6).

3.7. Diabetic mice show lower maximum membrane depolarization potentials than WT and DKO mice

Tetramethylrhodamine methyl ester was used to measure maximum membrane depolarization potential of SSM and IFM in each of the four groups, as described in Methods and Materials.

SSM and IFM from db/db mice showed lower maximum membrane depolarization potentials than WT and DKO SSM and IFM, respectively, as seen in Figures 3.7.2 and 3.7.3.

There were no significant differences seen in each of the test groups when comparing SSM and IFM, as shown in Figure 3.7.1.

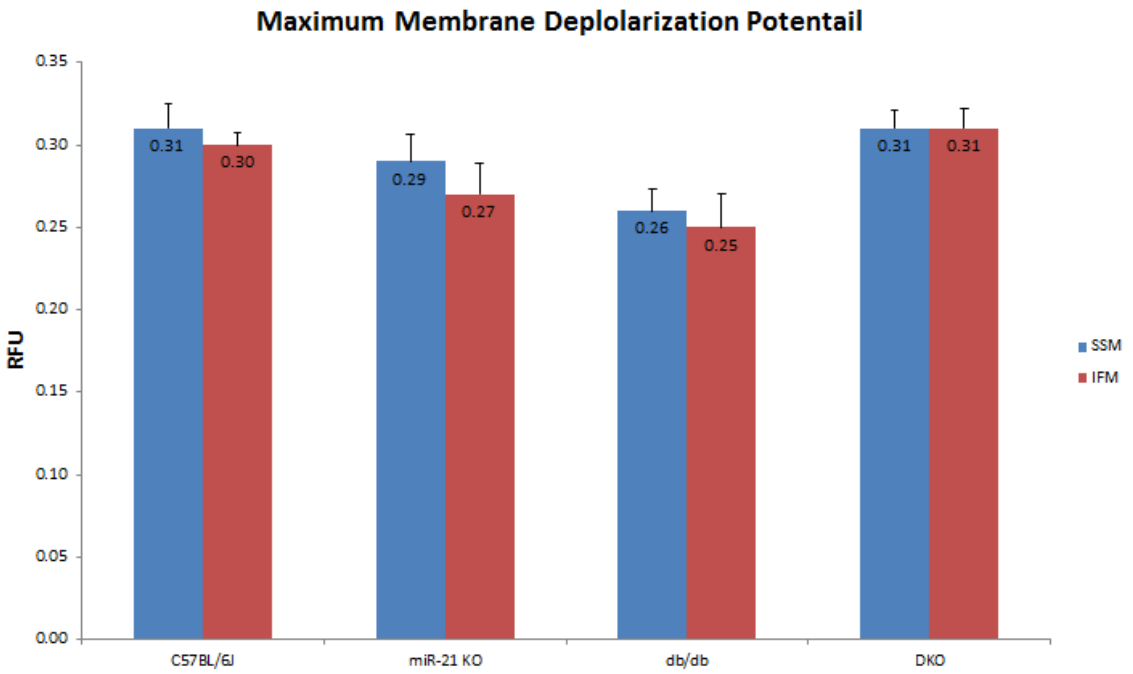

Figure 3.7.1. There were no significant differences in the maximum membrane depolarization potential when comparing SSM and IFM in of the separate test groups. A TMRM dye was used to measure maximum membrane potential of SSM and IFM in each of the four test groups. The depolarization potential was measured in units of RFU (Relative Fluorescence Units). The data is shown as mean ± SEM. A one way ANOVA was performed to compare the results. $P < 0.05$ for comparison between SSM and IFM (C57BL/6J n=5, miR-21 KO n=6, db/db n=4, DKO n=6).

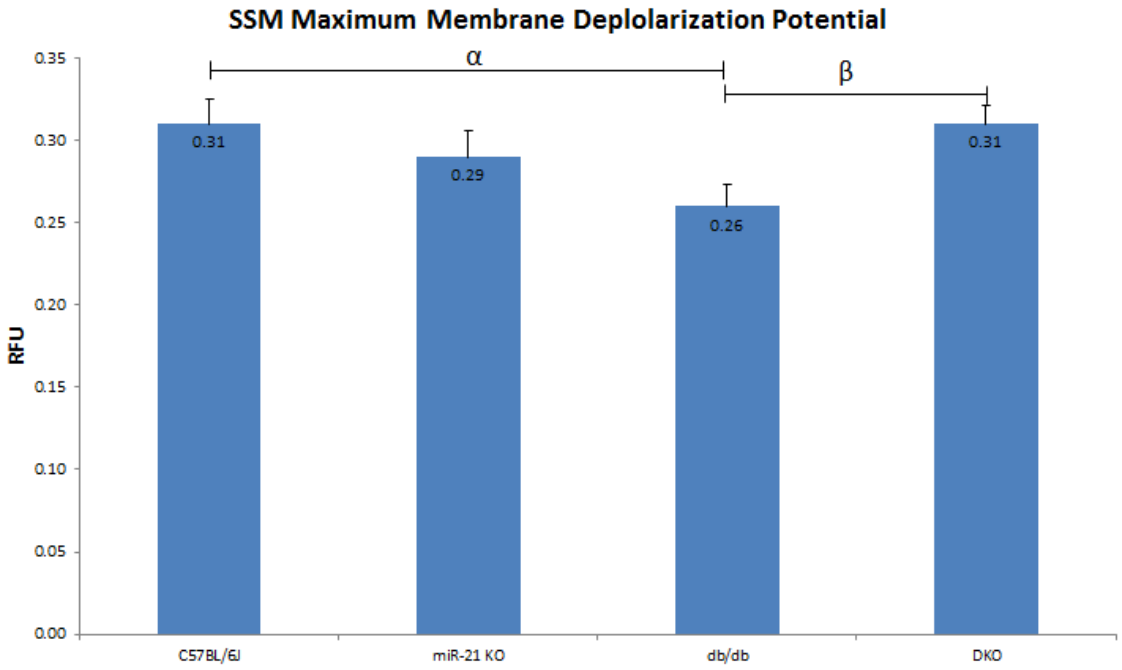

Figure 3.7.2. Db/db SSM had a lower maximum membrane depolarization potential than WT SSM and DKO SSM. A TMRM dye was used to measure membrane depolarization potential of SSM in each of the four test groups according to the procedure described in Methods and Materials. The depolarization potential was measured in units of RFU (Relative Fluorescence Units). The data is shown as mean ± SEM. A one way ANOVA was performed to compare the results. $^{\alpha}P < 0.05$ C57BL/6J vs. db/db and $^{\beta}P < 0.05$ db/db vs. DKO (C57BL/6J n=5, miR-21 KO n=6, db/db n=4, DKO n=6).

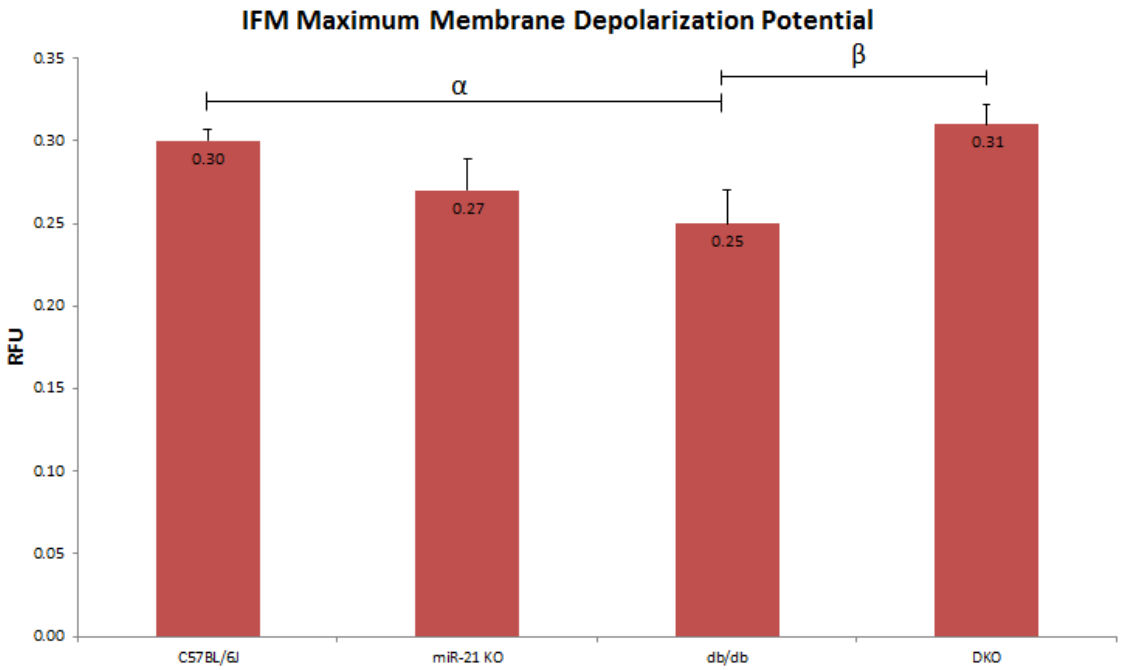

Figure 3.7.3. Db/db IFM had a lower maximum membrane depolarization potential than WT IFM and DKO IFM. A TMRM dye was used to measure membrane depolarization potential of SSM in each of the four test groups according to the procedure described in Methods and Materials. The depolarization potential was measured in units of RFU (Relative Fluorescence Units). The data is shown as mean ± SEM. A one way ANOVA was performed to compare the results. $^{\alpha}P < 0.05$ C57BL/6J vs. db/db and $^{\beta}P < 0.05$ db/db vs. DKO (C57BL/6J n=5, miR-21 KO n=6, db/db n=4, DKO n=6).

3.8. Maximal Complex I ROS production was increased in DKO SSM compared to the other test groups while DKO IFM Complex I ROS production was increased compared to C57BL/6J and db/db mice.

To measure ROS production in SSM and IFM in the four test groups, the amount of H_2O_2 release was quantified, as described in Methods and Materials. The ROS production of Complex I was increased in DKO SSM compared to C57BL/6J, miR-21 KO and db/db SSM. DKO IFM also showed an increase in ROS production compared to C57BL/6J and db/db IFM, as seen in Table 3.8.1.

Maximal Production of ROS in Complex I

	SSM	IFM
C57BL6/J	144.8 ± 18.4 $^{\alpha 1}$	100.3 ± 13.6 $^{\beta 1}$
miR-21 KO	150.1 ± 12.1 $^{\alpha 2}$	203.8 ± 58.8
db/db	137.6 ± 10.1 $^{\alpha 3}$	83.9 ± 13.9 $^{\beta 2}$
DKO	191.5 ± 7.8	138.0.3 ± 9.0

Table 3.8.1. DKO SSM had higher ROS production than the other three test SSM groups and DKO IFM had higher ROS production than C57BL/6J and db/db IFM. H_2O_2 release was measured and used as a marker when measuring ROS production in SSM and IFM of the four test groups, as described in Methods and Materials. The measurement unit was pmol/mg/min and the data is shown as mean ± SEM. A one way ANOVA was performed to compare the results. $^{\alpha 1}P < 0.05$ C57BL/6J SSM vs. DKO SSM, $^{\alpha 2}P < 0.05$ miR-21 KO SSM vs. DKO SSM, $^{\alpha 3}P < 0.05$ db/db SSM vs. DKO SSM, $^{\beta 1}P < 0.05$ C57BL/6J IFM vs. DKO IFM, and $^{\beta 2}P < 0.05$ db/db IFM vs. DKO IFM (C57BL/6J n=5, miR-21 KO n=6, db/db n=4, DKO n=6).

Chapter 4: Discussion

4.1. Db/db mice have the highest blood glucose levels but DKO blood glucose levels are similar to WT and miR-21 KO mice.

In mice, normal blood glucose levels are regarded to be approximately 100 mg/dl and diabetic blood glucose levels are 200 mg/dl and above (Keren et al., 2000). Since db/db mice display a model of type 2 diabetes mellitus, it is expected that they would show increased blood glucose levels. But knocking out miR-21 in diabetic mice restored the blood glucose levels back to values near WT and miR-21 KO levels, indicating that knocking out miR-21 may have a protective effect against hyperglycemia.

4.2. Knocking out miR-21 generally restores oxidative phosphorylation activity in diabetic mice

Oxidative phosphorylation is the term used to combine the activities of the electron transport chain (ETC) and ATP synthase function. Together, the transfer of electrons is linked to ATP production. This can be referred to as coupled respiration; electrons are transferred through Complex I, II, III, and IV and are eventually used to reduce oxygen to water. While the electrons are being transferred through the ETC, protons are translocated from the mitochondrial matrix to the inner mitochondrial space. This electrochemical potential drives Complex V, or ATP Synthase, to phosphorylate ADP and produce ATP. Coupled respiration rates measure the activity of Complexes I through Complex V, since ATP is linked with oxygen consumption. An uncoupling molecule, such as DNP, can disrupt the electrochemical

gradient of H^+ by allowing free movement of protons from the IMS to the matrix. So in uncoupled respiration, oxygen consumption is not linked with ATP production, as ATP Synthase activity is minimal. This diminishes Complex V function so only the activity of the electron transport chain is measured (Cox & Nelson, 2000).

There are many different ways to assess oxidative phosphorylation function including measuring State 3 respiration, State 4 respiration, respiratory control ratios, ADP:O ratios, maximum coupled respiration rates, and maximum uncoupled respiration rates. State 3 respiration is the respiration rate that occurs after mitochondria, substrates, and ADP have been added. When ADP is added, oxidative phosphorylation begins and oxygen consumption is measured. When the exogenous ADP has been phosphorylated, oxygen consumption slows and this is referred to as State 4 respiration. The respiratory control ratio (RCR) is just the ratio of State 3 respiration to State 4 respiration. A high RCR value shows that there was a large increase in oxygen consumption, an indicator of overall respiration, followed by a steady value of State 4 respiration, which suggests that the IMM is relatively intact and there is little proton "leakage" across the membrane. The ADP:O ratio refers to the amount of ADP molecules that are phosphorylated for each oxygen atom that is reduced to water. When a high concentration of ADP is added, the maximal rate of coupled respiration can be measured. The addition of DNP causes uncoupling of respiration from ATP production so only oxygen consumption can be measured (Lesnefsky & Hoppel, 2006). For Complex I, the substrates used were glutamate+malate while the substrates used for Complex II and Complex IV were succinate+rotenone and TMPD, respectively. Rotenone blocks the transfer of

electrons from Complex I to Complex II, which effectively allows for the measurement of the ETC only from Complex II through Complex V. The function of TMPD is to reduce cytochrome c, therefore mimicking the activity of Complex IV.

In the present data, the overall trend in Complex I and Complex II was that db/db mice had lower rates of oxygen consumption in the measured variables, for both SSM and IFM, than WT mice. This result is in accordance with literature as other studies have reported that db/db mice show lower respiration rates of Complex I and Complex II (Croston et al., 2014). But in the DKO mice, with a few exceptions due to statistical insignificance, higher levels of Complex I and Complex II were seen when compared to db/db mice in terms of State 3 respiration, maximum coupled respiration, and maximum uncoupled respiration in both the SSM and IFM populations. However, a significant difference between the maximum coupled respiration rates using substrates for Complex IV were not seen, indicating that a defect, if one is present, is upstream of Complex IV. Overall, this data indicates that knocking out miR-21 in diabetic mice has a protective effect on oxidative phosphorylation activity in cardiac mitochondria.

4.3. IFM show a greater ability for handling calcium than SSM in db/db mice

In some pathological conditions, the mitochondrial permeability transition pore can open, which leads to release of certain molecules that can cause mitochondrial death (Crompton, 1999). Calcium retention capacity can be used an assay to mark MPTP opening since a high concentration of calcium can lead to MPTP opening. A higher sensitivity to calcium indicates that the mitochondria is not able

to sequester much calcium and reaches MPTP opening earlier (Hollander, Thapa, & Sheperd, 2014).

In this study, the only significant difference was seen in the db/db mouse group, in which IFM showed the ability to handle calcium better than SSM. Due to high variability in the other groups, not many significant conclusions can be drawn even though the overall trend is that that knocking out miR-21 has a detrimental effect on calcium handling ability and IFM can handle calcium better than SSM in all four groups. The ability of IFM to handle calcium better has been reported in the literature and led to a slower opening of the MPTP (Hollander, Thapa, & Sheperd, 2014). However, these results cannot be taken at face value due to the high variability and low sample size.

4.4. DKO mice have higher depolarization and maximum membrane depolarization potentials compared to other db/db mice

As discussed earlier, oxidative phosphorylation generates a proton motive force (pmf) that contributes to ATP synthesis by Complex V of the respirasome and also creates a potential difference across the inner mitochondrial membrane (IMM). This potential can be measured using TMRM, which is a positively charged fluorescent dye that accumulates in the negatively charged matrix of the mitochondria. When mitochondria depolarize, TMRM is released and the fluorescence can be quantified. The depolarization potential can be measured when protons cross the IMM and are used by Complex V to make ATP from ADP. The maximum membrane potential can be measured using oligomycin and DNP.

Oligomycin is an inhibitor of Complex V and therefore stops the flow of protons across the IMM, which restores the mitochondrial membrane potential. DNP, an uncoupler, causes protons to flow across the IMM independently of Complex V function. Taking the difference between the oligomycin potential and final DNP potential results in the maximum membrane potential, as seen in Figure 4.4.1 (Chen, Ross, Hu, & Lesnefsky, 2012). Since the electrochemical potential across the IMM has an integral role in the activity of Complex V, it is expected that the IMM membrane potential has a large impact on oxidative phosphorylation rates.

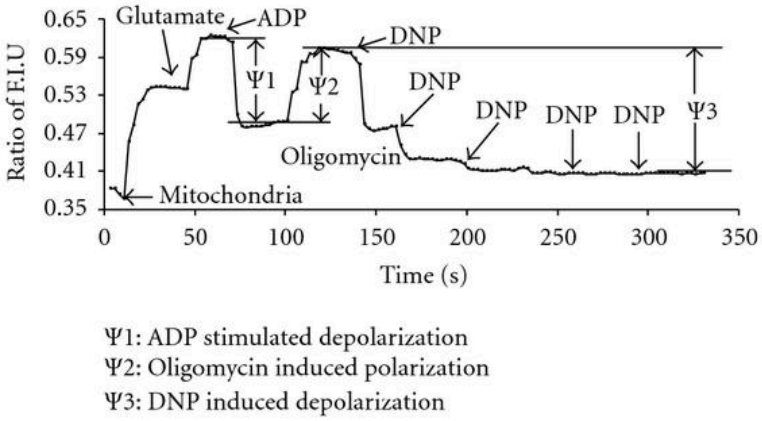

Figure 4.4.1. A depiction of depolarization and maximum membrane depolarization potential measurements (Chen, Ross, Hu, & Lesnefsky, 2012).

In this study, the DKO SSM and IFM populations both had higher depolarization potentials and higher membrane potentials than db/db mice. When the proton-motive force in intact, oxygen consumption increases as the membrane

potential increases in a nonlinear fashion. When the proton-motive force is depleted, oxygen consumption again increases with the membrane potential but in a linear fashion and at a much lower rate, as seen in Figure 4.4.2 (Jastroch, Divakaruni, Mookerjee, Treberg, & Brand, 2010).

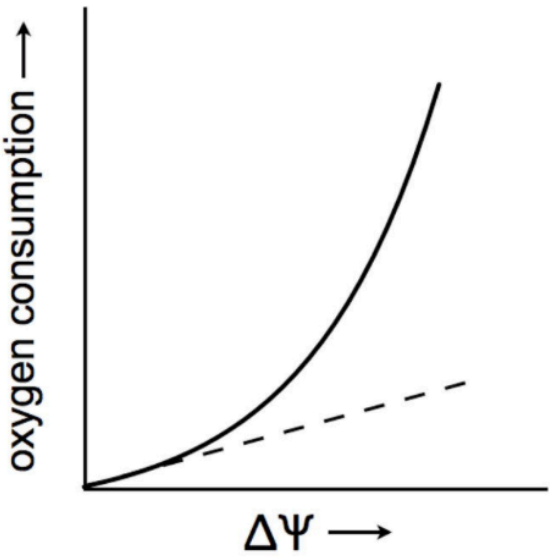

Figure 4.4.2. A depiction of the rise in oxygen consumption as the membrane potential increases. The solid line indicates the rise in oxygen consumption when the proton motive force is intact. The dashed line indicates the rise in oxygen consumption if the proton motive force is depleted (Jastroch, Divakaruni, Mookerjee, Treberg, & Brand, 2010).

Proton "leakage" from the IMM can be determined using oligomycin; since oligomycin blocks the movement of protons by Complex V, the membrane potential is restored. If there is a significant proton leak across the membrane, the membrane potential will be diminished. Since a depletion of membrane potential was not seen

with oligomycin in this study, it can be inferred that there was no significant proton backflow. This indicates that the proton motive force was intact and the rates of oxygen consumption were significant in the ETC. This is supported by the previously shown data references the rates of oxygen consumption in Complex I, Complex II, and Complex IV.

4.5. DKO production of ROS in both SSM and IFM was increased compared to most other groups

The overproduction of reactive oxygen species in cells is a poor indicator of overall cell survival as ROS production can lead to apoptosis and MPTP opening, both of which lead to cell death. However, it has been shown that at moderate concentrations, ROS can stimulate signaling cascades and lead to the activation of transcription, gene expression, and even muscle contraction. Muscle contraction is dependent on Ca^{2+} release from the sarcoplasmic reticulum, which might be partially regulated by the release of H_2O_2. (Suzuki, 1999).

In this study, H_2O_2 release was taken as a measure of ROS production in SSM and IFM in all four test groups. Glutamate and malate were used as substrates while rotenone was used to block the transfer of electrons from Complex I to Complex II, effectively giving a reliable measurement of the ROS production from only Complex I. With some exceptions due to statistical insignificance, the overall trend was that DKO mice showed increased ROS production in both SSM and IFM populations in Complex I.

These results may be an indicator that knocking out miR-21 in diabetic mice negatively impacts Complex I and leads to higher release of H_2O_2. However, knocking out miR-21 in the diabetic state led to an increase in oxidative phosphorylation Complex I function. The increased ROS production may play a role in the rescue of ATP production, as seen in the increased oxidative phosphorylation rates, which could lead to increased contractile function. Prioritizing oxidative phosphorylation function over ROS production could lead to these results and rescue contractile function but increased ROS production may affect the heart detrimentally in the long run.

Chapter 5: Conclusion

In this study, we hoped to determine some of the effects that miR-21 might have on subsarcolemmal and interfibrillar mitochondria in the normal and diabetic heart and hypothesized that knocking out miR-21 function would have a positive impact on oxidative phosphorylation activity, ROS production, and MPTP opening. We saw that knocking out miR-21 had both positive and negative effects based on what variable was being measured and in which group it was being tested.

Complex I is especially important in oxidative phosphorylation because it is NADH-dependent. It uses the electrons from NADH to set off the oxidative phosphorylation chain. NADH is the link between the catabolism of proteins, sugars, and fats, and eventual energy production as the breakdown of those molecules creates substrates that enter the citric acid cycle and eventually, electrons are transferred to NADH. Glucose oxidation and fatty oxidation both use NADH as an

intermediary between catabolism and ATP production from oxidative phosphorylation (Cox & Nelson, 2000).

Knocking out miR-21 in diabetic mice increased function in Complex I and Complex II. However, DKO mice also showed increased ROS production in Complex I.

Overall, these results indicate that knocking out miR-21 may have a protective role in oxidative phosphorylation function in the diabetic heart but may come at the expense of increased ROS production so the initial hypothesis may be partially correct.

Due to small sample size, few solid conclusions can be drawn even though the overall trend is present throughout the measured variables. Increasing the sample size might improve the efficacy of the measured variables and could be a step to take in the future. This study also raises further questions and avenues for exploration, such as if miR-21 primarily has a systemic effect on diabetic mice and then a secondary effect on diabetic heart function. In the long term, mitochondria from the liver and skeletal muscle could be tested for function and compared against cardiac mitochondrial data. It might be particularly beneficial to check the effects of knocking out miR-21 in the pancreas, especially in the insulin producing cells, as a total knockout of miR-21 had a protective effect against hyperglycemia in diabetic mice. In the short term, the sample size could be increased to improve the significance of the present data. Future studies should be performed to pinpoint the exact effects miR-21 has on the heart, as well as throughout the body.

Literature Cited

Aluri, H., Koka, S., Lesnefsky, E., Kukreja, R. (2012). Chronic treatment with the long acting phosphodiesterase-5 inhbitor, tadalafil, decreases mitochondrial damage in diabetic mice. *Mitochondrion*. (*12*: 5, p. 576). doi: 10.1016/j.mito.2012.07.067

Asangani, I., Rasheed, S., Nikolova, D., Leupold, J., Colburn, N.,…,Allgayer, H., (2008). MicroRNA-21 (miR-21) post-transcriptionally downregulates tumor suppressor Pdcd4 and stimulates invasion, intravasation, and metastasis in colorectal cancer. *Oncogene*. (*27*, pp. 2128-2136). doi: 10.1038/sj.onc.1210856

Baumgartner, H., Gerasimenko, J., Thorne, C., Ferdek, P., Pozzan, T.,…, Gerasimenko, O. (2009). Calcium elevation in mitochondria is the main Ca^{2+} requirement for mitochondrial permeability transition pore (MPTP) opening. *The Journal of Biological Chemistry*. (284, 20796-20803). doi: 10.1074/jbc.M109.025353

Belke, D., Severson., D. (2012). Diabetes in mice with monogenic obesity: the db/db mouse and its use in the study of cardiac consequences. In Joost, H-G., Al-Hasani, H., Schurmann, A (Eds.), *Animal Models in Diabetes Research* (pp. 47-59). New York, Springer.

Boudina, S., Abel, E. (2010). Diabetic cardiomyopathy, causes and effects. *Reviews in Endocrine and Metabolic Disorders*. (*11*, pp. 31-39). doi: 10.1007/s11154-010-9131-7

Bugger, H., Abel, E. (2014). Molecular mechanisms of diabetic cardiomyopathy. *Diabetologia*. 57:660-671. DOI 10.1007/s00125-014-3171-6

Chen, Q., Camara, A., Stowe, D., Hoppel, C., Lesnefsky, E. (2007). Modulation of electron transport protects cardiac mitochondria and decreases myocardial injury during ischemia and reperfusion. *American Journal of Physiology – Cell Physiology*. (*292*:1, pp C137-C147). doi: 10.1152/ajpcell.00270/2006

Chen, Q., Xu, H., Xu, A., Ross, T., Bowler, E., Hu, Y., Lesnefsky, E. (2015). Inhibition of Bcl-2 sensitizes mitochondrial permeability transition pore (MPTP) opening in ischemia-damaged mitochondria. *PLOS One*. (*10*:3). doi: 10.1371.journal.pone.0118834

Chen, Q., Moghaddas, S., Hoppel, C., Lesnefsky, E. (2008). Ischemic defects in the electron transport chain increase the production of reactive oxygen species from isolated rat heart mitochondria. *American Journal of Physiology – Cell Physiology*. (*294*: 2, pp C460-C466). doi: 10/1152/ajpcell.00211.2007

Chen, Q., Ross, T., Hu, Y., Lesnefsky, E. (2012). Blockade of electron transport at the onset of reperfusion decreases cardiac injury in aged hearts by protecting the inner mitochondrial membrane. *Journal of Aging Research*. (12). doi: 1.1155/2012/753949

Cheng, Y., Zhang, C. (2010). MicroRNA-21 in Cardiovascular Disease. *Journal of Cardiovascular Translational Research*. (*3*, pp. 251-255). doi: 10.1007/s12265-010-9169-7

Clark, L. (2007). *Cardiovascular Disease and Diabetes*. New York NY: McGraw Hill

Cox, M. M., & Nelson, D.L. (2000). Major Structural Features of Eukaryotic Cells (pp. 36). In *Lehninger Principles of Biochemistry* (3rd Ed.). New York, NY: Worth

Cox, M. M., & Nelson, D.L. (2000). Oxidative Phosphorylation and Photophosphorylation(pp. 659-685). In *Lehninger Principles of Biochemistry* (3rd Ed.). New York, NY: Worth

Crompton, M. (1999). The mitochondrial permeability transition pore and its role in cell death. *Biochemistry Journal*. (*341*: 2, pp 243-249).

Croston, T., Thapa, D., Holden, A., Tveter, K., Lewis, S.,...Hollander, J. (2014). Functional deficiencies of subsarcolemmal mitochondria in the type 2 diabetic human heart. *American Journal of Physiology - Heart and Circulatory Physiology*. (*307*:1, pp H54-H65). doi: 10.1152/ajpheart.00875.2013

Dey, N., Das, F., Mariappan, M., Mandal, C., Choudhury, N.,..., Choudhury, G. (2011). MicroRNA-21 Orchestrates High Glucose-induced Sigmals to TOR Complex 1, Resulting in Renal Cell Pathology in Diabetes. *The Journal of Biological Chemistry*. (*286*:29, pp. 25586-25603). doi: 10.1074/jbc.M110.208066

Hollander, J., Thapa, D., Sheperd, D. (2014). Physiological and structural differences in spatially distinct subpopulations of cardiac mitochondria: influence of cardiac pathologies. *American Journal of Physiology - Heart and Circulatory Physiology*. (*307*:1, pp H1-H14). doi: 10.1152/ajpheart.00747.2013

Jastroch, M., Divakaruni, A., Mookerjee, S., Treberg, J., Brand, M. (2010). Mitochondrial proton and electron leaks. *Essays in Biochemistry*. (47, pp. 53-67). doi: 10.1042/bse0470053

Keren, P., George, J., Shaish, A., Levkovitz, H., Janakovic, Z,..., Harats, D. (2000). Effect of hyperglycemia and hyperlipidemia on atherosclerosis in LDL receptor-defecient mice: establishment of a combined model and association with heat shock 65 immunity. *Diabetes*. (*49*: 6, pp 1064-1069). doi: 10.2337/diabetes.49.6.1064

Kumar, A., Raut, S., Saika, U., Sharma, R., Khullar, M. (2011). Abstract 15227: Microrna-21 contributes to diabetic cardiomyopathy associated cardiac fibrosis. *Circulation*. (124).

Lesnefsky, E., Hoppel, C. (2006). Oxidative phosphorylation and aging. *Ageing Research Reviews*. (*5*:4, pp 402-433). doi: 10.1016/j.arr.2006.04.001

Iorio, M., Ferracin, M., Liu, C., Veronese, A., Spizzo, R.,…,Croce, C., (2005). MicroRNA Gene Expression Deregulation in Human Breast Cancer. *Cancer Research*. (*65:*7065). doi: 10.1158/0008-5472.CAN-05-1783

Marin-Garcia, J. (2013). The Energy-Consuming Heart(pp. 3-11). In *Mitochondria and Their Role in Cardiovascular Disease*. New York, NY: Springer

McClelland, A., Edelstein, M., Komers, R., Jha, J., Winbanks, C.,…, Cooper, M. (2015). miR-21 promotes renal fibrosis in diabetic nephropathy by targeting PTEN and SMAD7. *Clinical Science*. (*129*: 12, pp. 1237-1249). doi: 10.1042/CS20150427

Melmed, S., Polonsky, K., Larsen, P., Kronenberg, H. (2011). Type 2 Diabetes Mellitus. *Williams Textbook of Endocrinology* (pp. 1371-1436). Philadelphia, PA: Saunders.

Mollica, M., Lionetti, L., Crescenzo, R., D'Andrea, E., Ferraro, M., Liverini, G., Iossa, S. (2006). Heterogeneous bioenergetic behaviour of subsarcolemmal and intermyofibrillar mitochondria in fed and fasted rats. *Cellular and Molecular Life Sciences*. (*63:*3, pp. 358-366).

National Institute for of Diabetes and Digestive and Kidney Diseases. (2014). *Cause of Diabetes*. National Institutes of Health.

Palmer, J., Tandler, B., Hoppel, C. (1977). Biochemical Properties of Subsarcolemmal and Interfibrillar Mitochondria Isolated from Rat Cardiac Muscle. *The Journal of Biological Chemistry*. (*252:*23, pp. 8731-8739).

Patrick, D., Montgomery, R., Qi, X., Obad, S., Kauppinen, S.,..., Olsen, E. (2010). Stress-dependent cardiac remodeling occurs in the absence of microRNA-21 I mice. *Journal of Clinical Investigation*. (*120*:11, pp 3912-3916). doi: 10.1172/JCI43604

Ross, T., Szczepanek, K., Bowler, E., Hu, Y., Larner, A.,...,Chen, Q. (2013). Reverse electron flow-mediated ROS generation in ischemia damaged mitochondria: role of complex I inhibition vs. depolarization of inner mitochondrial membrane. *Biochimica et Biophysica Acta*. (*1830*: 10, pp 4537-4542). doi: 10.1016/j.bbagen.2013.05.035

Scaduto, R., Grotyohann, L. (1999). Measurement of mitochondria membrane potential using fluorescent rhodamine derivatives. *Biophysics Journal*. (*76*: 1, pp. 469-477). Doi: 10.1016/S00006-3495(99)77214-0

Sekar, D., Venugopal, B., Sekar, P., Ramalingam, K. (2016). Role of microRNA 21 in diabetes and associated/related diseases. *Gene*. (*582*: 1, pp. 14-18). doi: 10.1016/j.gene.2016.01.039

Suzuki, Y., Ford, G. (1999). Redox regulation of signal transduction in cardiac and smooth muscle. *Journal of Molecular and cellular Cardiology*. (*31*:2, pp. 345-353). doi: 10.1006/jmcc.1998.0872

Szabo, Csaba. (2012). Roles of hydrogen sulfide in the pathogenesis of diabetes mellitus and its complications. *Antioxidants & Redox Signaling*. (*17*:1, pp 68-80). doi: 10.1089/ars.2011.4451

Thum, T., Gross, C., Fiedler, J., Fischer, T., Kissler, S.,…, Engelhardt, S. (2008). MicroRNA-21 contributes to myocardial disease by stimulating MAP kinase signaling in fibroblasts. *Nature*. (*456*: 18). doi: 10.1038/nature07511

Toldo, S., Das, A., Mezzaroma, E., Chau, V., Marchetti, C.,…, Salloum, F. (2014). Induction of MicroRNA-21 with Exogenous Hydrogen Sulfide Attenuates Myocardial Ischemic and Inflammatory Injury in Mice. *Circulation: Cardiovascular Genetics*. (*7*, pp. 311-320). doi: 10.1161/CIRCGENETICS.113.000381

Tu, Y., Wan, L., Fan., Wang, K., Bu, L.,…,Shen, B. (2013). Ischemic Postconditioning-Mediated miRNA-21 Protects against Cardiac ischemia/reperfusion injury via PTEN/Akt pathway. *PLoS One*. (*8*:10) doi: 10.1371/journal.pone.0075872

Volina, S., Calin, G., Liu, C., Ambs, S., Cimmino, A.,…Croce, C., (2006). A microRNA expression signature of human solid tumors defines cancer gene targets. *Proceedings of the National Academy of Sciences of the United States of America*. (*103*: 7, pp. 2257-2261). doi: 10.1073/pnas.0510565103

Williamson, C., Dabkowski, E., Baseler, W., Croston, T., Alway, S., Hollander, J. (2010). Enhanced apoptotic propensity in diabetic cardiac mitochondria: influence of subcellular spatial location. *American Journal of Physiology – Heart and Circulatory Physiology*. (*298*:2). doi: 10.1152/ajpheart.00668.2009

Wong, R., Steenbergen, C., Murphy, E. (2012). Mitochondrial permeability transition pore and calcium handling. *Methods of Molecular Biology*. (810, pp 235-242). doi: 10.1007/978-1-61779-382-0_15

Zhong, X., Chung, A., Chen, H., Dong, Y., Meng, X.,..., Lan, H. (2013). miR-21 is a key therapeutic target for renal injury in a mouse model of type 2 diabeties. *Diabetologia*. (*56*: 3, pp. 663-674). doi: 10.1007/s00125-012-2804-x